Predicting Post-Wildfire Stream Temperature and Turbidity: A Machine Learning Approach in Western U.S. Watersheds

Junjie Chen [ID] and Heejun Chang *[ID]

Department of Geography, Portland State University, Portland, OR 97201, USA; junchen@pdx.edu
* Correspondence: changh@pdx.edu

Abstract: Wildfires significantly impact water quality in the Western United States, posing challenges for water resource management. However, limited research quantifies post-wildfire stream temperature and turbidity changes across diverse climatic zones. This study addresses this gap by using Random Forest (RF) and Support Vector Regression (SVR) models to predict post-wildfire stream temperature and turbidity based on climate, streamflow, and fire data from the Clackamas and Russian River Watersheds. We selected Random Forest (RF) and Support Vector Regression (SVR) because they handle non-linear, high-dimensional data, balance accuracy with efficiency, and capture complex post-wildfire stream temperature and turbidity dynamics with minimal assumptions. The primary objectives were to evaluate model performance, conduct sensitivity analyses, and project mid-21st century water quality changes under Representative Concentration Pathway (RCP) 4.5 and 8.5 scenarios. Sensitivity analyses indicated that 7-day maximum air temperature and discharge were the most influential predictors. Results show that RF outperformed SVR, achieving an R^2 of 0.98 and root mean square error of 0.88 °C for stream temperature predictions. Post-wildfire turbidity increased up to 70 NTU during storm events in highly burned subwatersheds. Under RCP 8.5, stream temperatures are projected to rise by 2.2 °C by 2050. RF's ensemble approach captured non-linear relationships effectively, while SVR excelled in high-dimensional datasets but struggled with temporal variability. These findings underscore the importance of using machine learning for understanding complex post-fire hydrology. We recommend adaptive reservoir operations and targeted riparian restoration to mitigate warming trends. This research highlights machine learning's utility for predicting post-wildfire impacts and informing climate-resilient water management strategies.

Keywords: wildfires; stream temperature; turbidity; random forest; support vector regression

1. Introduction

Wildfires have become an increasingly significant environmental concern, particularly in the Western United States, where they profoundly impact water quality. The removal of vegetation and organic matter by wildfires exposes soil to erosional forces, leading to heightened levels of sediment, nutrients, and organic matter in water bodies [1]. Many forested watersheds in this region provide high-quality drinking water to residents and are extremely vulnerable to unprecedented wildfires that have occurred in recent decades. Changes in wildfire frequency, size, and burn area have altered watershed hydrology by increasing runoff, decreasing infiltration, and raising the risks of debris flows, ultimately deteriorating water quality [2,3]. These post-wildfire impacts on hydrology can be exacerbated by atmospheric rivers, peak flows, and subsequent re-burns [4,5]. The cumulative

effects necessitate a comprehensive approach to water quality monitoring and management in wildfire-prone regions.

Increased stream temperature and turbidity are among the most critical consequences of wildfires, posing severe challenges for aquatic ecosystems and water treatment processes [1]. Elevated stream temperatures, resulting from increased solar radiation due to the loss of canopy cover, can reduce dissolved oxygen levels, stressing aquatic life and altering ecosystem functions [6]. These temperature increases can disrupt the metabolic rates of fish and other aquatic organisms, leading to decreased populations of sensitive species [2]. Riparian shading is a critical control on stream temperature, as it limits direct solar radiation and helps maintain cooler water conditions essential for aquatic ecosystem health [1]. In wildfire-affected watersheds, the degree of riparian vegetation loss can lead to increased stream temperatures, especially in reaches where high burn severity reduces canopy cover. Burn severity classes and riparian buffer burn areas are often examined to quantify shading loss, recognizing that the impacts on stream temperature are spatially dependent. Localized increases in temperature can be significant in heavily burned areas, but downstream effects are often muted unless a substantial portion of the riparian zone across the watershed is affected. Additionally, post-fire hydrology can exacerbate turbidity levels due to increased sediment transport during storm events, as documented in studies of Western U.S. rivers [3]. By including burn severity metrics, our analysis captures how riparian loss and watershed-scale burn dynamics interact to influence post-fire stream thermal regimes and sediment fluxes, emphasizing the need for spatially explicit water resource management strategies to mitigate post-fire water quality degradation. Furthermore, the influx of ash, sediments, and organic debris significantly raises turbidity levels [7], necessitating more extensive filtration and chemical treatments in drinking water plants, increasing operational costs and complicating efforts to maintain water quality standards [8,9]. These changes have significant implications for both aquatic health and drinking water treatment, underscoring the need for effective management strategies in wildfire-affected areas.

Predicting stream temperature and turbidity and assessing their relationships with explanatory variables such as climatic and streamflow variables has traditionally relied on empirical and deterministic models. Empirical models often use statistical techniques to correlate stream temperature and turbidity with air temperature, precipitation, and discharge rates [10]. Linear regression models, for instance, have been widely used due to their simplicity and ease of interpretation, allowing researchers to establish direct relationships between environmental variables and stream conditions [11]. However, these models may struggle with non-linear relationships and interactions among predictors.

Deterministic models, such as those based on heat budget calculations, simulate the physical processes influencing stream temperature by accounting for energy exchanges between the stream and its environment [12,13]. These models are often more accurate but require extensive data and detailed parameterization, which can be challenging to obtain and validate. Additionally, models like the Soil and Water Assessment Tool (SWAT) and River Basin Model (RBM) integrate hydrological and meteorological data to predict streamflow and associated water quality parameters, including turbidity [14,15]. While these models provide comprehensive and detailed predictions, their complexity and data requirements can be major drawbacks, often necessitating substantial resources for data collection, calibration, and validation.

In recent years, machine learning techniques, such as Random Forest (RF) and Support Vector Regression (SVR), have emerged as powerful tools for assessing the relationships between climatic variables and water quality parameters when sufficient pre- and post-fire data are available. For instance, Kang et al. (2024) [16] utilized Random Forest models to explore the impacts of wildfires on streamflow in Western Oregon, demonstrating the

importance of burn severity as a predictor variable. Similarly, Rajesh and Rehana (2021) [17] employed SVR to predict water quality parameters in response to varying climatic conditions, highlighting the adaptability and robustness of these models in handling complex environmental data. Wade et al. (2023) [18] employ Random Forest models to identify the primary controls on river water temperature regimes in 410 watersheds spanning the conterminous United States, revealing that antecedent weather conditions, river discharge, and riparian vegetation significantly influence thermal dynamics. In contrast, Feigl et al. (2021) [19] compare various machine-learning methods, including support vector machines, random forests, and gradient boosting machines, finding that gradient boosting machines generally outperform others in predicting stream water temperatures. These models are capable of handling large, complex datasets and uncovering non-linear relationships that traditional methods might overlook [20–22]. These advanced models have demonstrated superior performance in various hydrological studies, marking a significant advancement over traditional empirical and deterministic approaches. Specifically, in the context of wildfire-affected watersheds, machine learning models can predict post-fire stream temperature and turbidity based on climatic factors such as air temperature, discharge, and precipitation [23].

This study's unique approach lies in its examination of two pairs of nested watersheds located in distinct geographical and climatic zones in Oregon and Northern California. By applying RF and SVR models across these diverse environments, we aim to understand the extent to which stream temperature and turbidity are associated with climatic variables such as air temperature, precipitation, and discharge. By comparing the performance of the two machine learning models, we can identify the most effective approach to projecting water quality changes. The performance of these models will provide critical insights into the dependency of stream temperature and turbidity on climatic factors. If the models perform poorly, it may indicate that other factors, such as landscape characteristics, vegetation cover, and soil types, have a more significant influence on stream conditions.

Objective 1 of our study is to assess the impact of air temperature, precipitation, and discharge on stream temperature and turbidity using RF and SVR models. By evaluating these relationships, we aim to determine the accuracy and reliability of these models in reflecting post-fire watershed conditions. Objective 2 is to apply these models to downscaled future climate data and project future stream temperature in mid-century climate scenarios under two Representative Concentration Pathways (RCPs). Integrating machine learning models with downscaled climate projections offers valuable insights into future water quality scenarios in wildfire-prone regions. By simulating the effects of climatic changes on stream temperature, these models can inform long-term water management strategies and help adapt to the impacts of climate change on water resources [24].

This study addresses the critical need for advanced predictive models capable of handling the complex non-linear interactions between multiple climatic and environmental variables influencing water quality in post-wildfire scenarios. By utilizing machine learning techniques, we aim to enhance the accuracy and reliability of water quality predictions, ultimately aiding in developing more resilient water management practices in regions susceptible to wildfires [20,23]. Furthermore, this research contributes to a broader understanding of the interconnectedness between climate change and increased wildfire activity, providing valuable insights for future environmental and water resource planning [25,26]. This holistic approach is essential for preparing and adapting to the evolving challenges posed by climate change and the rising frequency and intensity of wildfires [5,24].

2. Data and Methods

2.1. Study Site

For our study sites, we chose the Clackamas River Watershed in Oregon and the Russian River Watershed in Sonoma County, Northern California (Table 1). These two watersheds were chosen because they contain nested watersheds with different degrees of burning from recent wildfires. Additionally, these two watersheds provide primary drinking water resources to local communities. Finally, future climate change is likely to change the hydrology of these watersheds affecting stream temperature and turbidity, which will have negative impacts on aquatic ecosystems and human consumption of water.

Table 1. Study site, wildfire data summary, and major land cover types.

USGS Gauge ID	Drainage Area (km^2)	Gauge Name	Pre-Fire Data Period	Post-Fire Data Period	Fire Date	Percent Watershed Burned	% Urban	% Agri-cultural	% Forest	% Shrub/ Grassland
14210000	1738	CLACKAMAS RIVER AT ESTACADA, OR	2007– 2020	2020– 2024	2020	20	1.1	0.5	92	5.4
14211010	2435	CLACKAMAS RIVER NEAR OREGON CITY, OR	2007– 2020	2020– 2024	2020	17	4.3	6.8	81.7	5.8
11462500	938	RUSSIAN R NR HOPLAND CA	2007– 2017	2018– 2024	2017, 2018	14.4	7.7	4.2	29.8	57.2
11467000	3465	RUSSIAN R A HACIENDA BRIDGE NR GUERNEVILLE CA	2007– 2019	2021– 2024	2019, 2021	9.4	11.4	7.2	32.4	47.6

The Clackamas River Watershed, located in Northwest Oregon, covers an area of approximately 2435 km^2. It is characterized by a diverse climate with mild, wet winters and warm, dry summers, resulting in a significant amount of annual precipitation, particularly during the winter months. This precipitation pattern is crucial for the region's hydrology, contributing to the river's flow and the overall water availability in the watershed. The Clackamas River is a vital water source for local communities, providing drinking water for over 300,000 residents. Hydrologically, the Clackamas River Watershed includes several tributaries and features a range of elevations and geologic features, from lowland areas to mountainous regions in the Cascade Range. This topographical and geologic variation influences the watershed's hydrological processes, including runoff, infiltration, groundwater recharge, and sediment transport. Unlike higher-elevation watersheds in the Cascade Range that are influenced by glacial melt or perennial snowfields, the Clackamas River Watershed does not receive contributions from glaciers or consistent snowpack. Instead, its hydrology is driven primarily by rainfall, with only transient snow accumulation during winter months at higher elevations. As a result, the watershed's seasonal flow patterns are more sensitive to variations in precipitation and temperature rather than snowmelt or glacial dynamics.

The Clackamas River's baseflow is significantly influenced by the geology of its watershed, with substantial contributions from subsurface flow that help sustain streamflow during the dry summer months [27,28]. The Baseflow Index (BFI), which quantifies the proportion of streamflow derived from groundwater, reflects this groundwater influence, with the Estacada gauge showing a BFI of 71 and the Oregon City gauge reporting a slightly lower BFI of 66. These values indicate that a substantial portion of the river's flow originates from underground recharge, particularly from the highly permeable volcanic and sedimentary formations present in the upper watershed. Seasonal recharge patterns are governed by winter precipitation infiltrating through porous soils and recharging aquifers, which gradually release cooler water to the river during summer, helping to moderate stream temperatures. The land cover in the watershed is predominantly forested,

with coniferous forests, mixed woodlands, and riparian vegetation playing key roles in maintaining ecological balance. The watershed is heavily managed and houses several water reservoirs on the mainstem. The watershed is home to a diverse array of aquatic species, including threatened and endangered species such as the coho salmon, spring Chinook, and winter steelhead. These species rely on the river's cold, clear waters and healthy riparian habitats. Climate change is expected to alter streamflow patterns and increase water temperatures, potentially exacerbating stress on these sensitive species and further challenging water management strategies in the Clackamas River Watershed [27,28].

In September 2020, the Riverside Fire burned the southwestern edge of the upper watershed, growing to over 100,000 acres before being contained (Figure 1a). According to data obtained from the Monitoring Trends in Burn Severity (MTBS) database, the Riverside Fire burned at high severity for 37%, moderate severity for 20%, and low severity for 30%, with parts of the Clackamas River corridor and surrounding hillsides experiencing high fire intensity and impacts. The September fire has somewhat nuanced effects on hydrology, with no significant increases in runoff ratios and peak flows during the post-fire period [17,29].
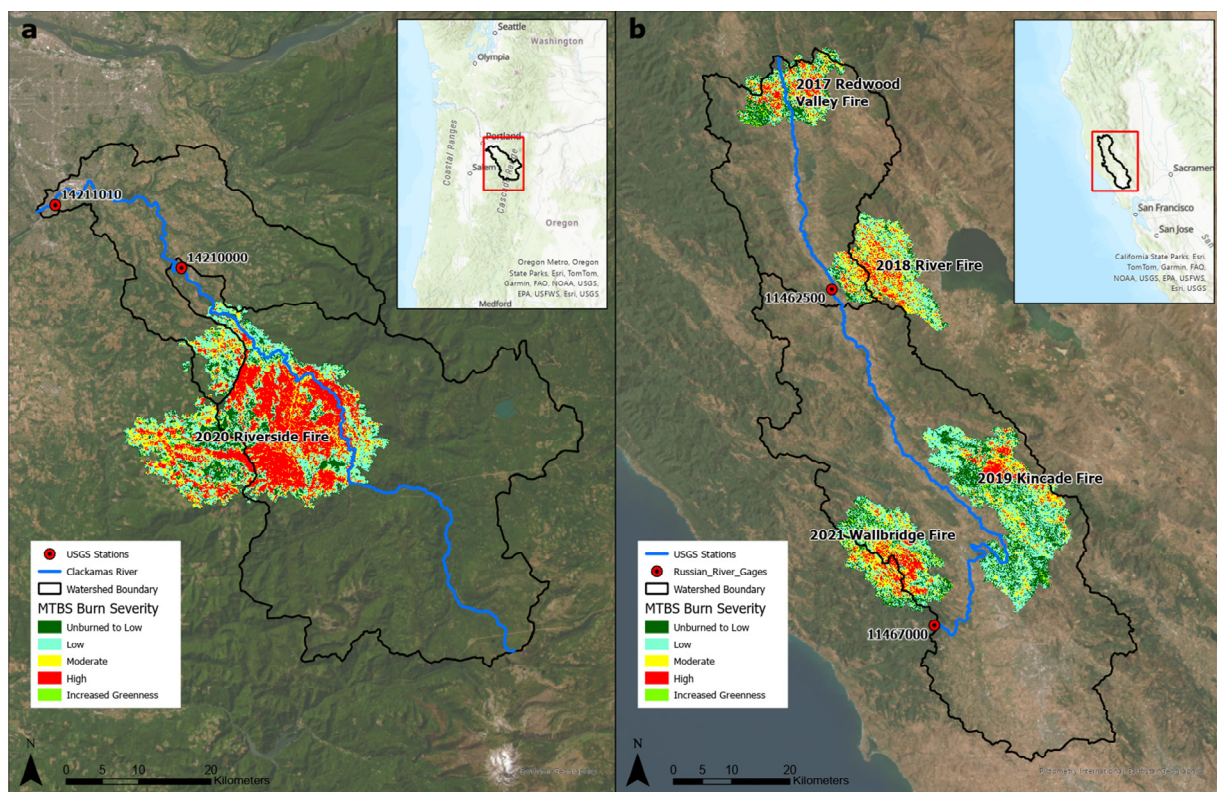
Figure 1. Study area map with USGS stream gage locations, watershed boundary and MTBS wildfire burn severity map for the Clackamas River Watershed (**a**) and Russian River Watershed (**b**).

Our second study site the Russian River Watershed, located in Northern California, spans approximately 3846 km^2, covering urban, agricultural, and forested lands in Sonoma and Mendocino counties. It experiences a Mediterranean climate with mild, wet winters and hot, dry summers, and the annual rainfall ranges from 730 to 1800 mm, primarily from large atmospheric river events [30]. This climate pattern substantially influences the watershed's hydrology, leading to both droughts and floods. The mainstem of the Russian River Watershed is characterized by alluvial valleys underlain by extensive bedrock of the Franciscan Complex, making it one of California's most flood-prone regions [31]. Land cover includes agricultural areas, evergreen forests, scrub/shrub, and grasslands,

supporting diverse habitats [32,33]. Significant water management infrastructure, such as Lake Mendocino and Lake Sonoma, is crucial for water supply and flood control, serving a population of 650,000.

The Russian River Watershed's hydrology is influenced by climatic variability, human activities, and land use, with the inter-basin transfer of water from the Eel River via the Potter Valley Project augmenting water availability during the dry season. Unlike snow-fed watersheds, the Russian River Watershed relies on seasonal rainfall, leading to high flows and elevated turbidity during winter storms and low flows with warmer stream temperatures in summer. Without snowmelt to sustain baseflows, summer flows depend on stored water and inter-basin transfers, making the watershed more vulnerable to drought and wildfire impacts on sediment loads and stream temperatures. The Russian River's baseflow is notably lower compared to the Clackamas River, reflecting the watershed's geology and seasonal hydrological patterns. The Baseflow Index (BFI) at the Hopland gauge is 36, while the Guerneville gauge has a slightly lower BFI of 34, indicating that groundwater contributions to streamflow are relatively limited. This is consistent with the region's geology, which is characterized by less permeable bedrock from the Franciscan Complex and alluvial deposits in the valleys that store and release water more episodically. Seasonal recharge primarily occurs during winter storms, but the watershed's Mediterranean climate and limited groundwater storage capacity result in reduced subsurface contributions during the dry summer months. Consequently, streamflow during the summer is more reliant on surface water and reservoir releases, contributing to warmer stream temperatures.

Recent wildfires have impacted the watershed, affecting sediment loads and water quality [11,34]. Management and restoration efforts focus on maintaining ecological and water supply resilience amidst these challenges [35]. Understanding these interactions is essential for developing effective water management and conservation strategies to ensure the resilience of this critical watershed. Between 2017 and 2020, four major wildfires burned in the Russian River Watershed, covering an area of over 1000 km^2 and roughly 28% of the total watershed area (Figure 1b). These wildfires occurred during a prolonged drought period, leading to widespread destruction of vegetation, increased sediment loads, and altered hydrological dynamics within the watershed [35].

2.2. Data Collection

We collected daily streamflow, stream temperature, and turbidity data from two long-term USGS National Water Information Systems (NWIS) streamgages within the Clackamas Watershed: one near Oregon City (#14211010) at the confluence with the Willamette River, and the other upstream at Estacada (#14210000), covering the period from October 2007 to June 2024. For the Russian River Watershed, we acquired long-term streamflow, turbidity, and stream temperature data from two USGS streamgages: one at Hacienda Bridge near Guerneville (#11467000) and one in a nested headwater sub-basin near Hopland (#11462500), covering the same period. Associated daily air temperature and precipitation data for both watersheds were obtained from Oregon State University's PRISM dataset [36]. All datasets were screened to ensure continuous data availability with no more than 30 days missing, requiring at least 10 years of pre-fire data and 3 years of post-fire data. In addition to climatic and hydrological variables, we included the percent of the watershed burned at different severity levels (low, moderate, and high) and percent burn area from the MTBS dataset to capture the potential impacts of wildfire on stream temperature and turbidity. Additionally, we collected the Multivariate Adaptive Constructed Analogs (MACA) downscaled climate dataset for the study area, which provides high-resolution climate projections by statistically downscaling global climate models to a spatial resolution of 4 km, offering detailed and regionally specific climate information [37].

2.3. Predictor Variables

Air temperature significantly impacts stream temperature, with increased air temperatures leading to higher stream temperatures, adversely affecting aquatic ecosystems by reducing dissolved oxygen levels and stressing aquatic life [38,39]. This relationship highlights the importance of including air temperature as a key variable in predictive models to forecast stream temperature changes accurately, particularly in post-wildfire scenarios [40]. To enhance our predictions' accuracy and relevance, we tested several air temperature metrics for sensitivity in our machine learning models, as shown in Table 2. These metrics include mean daily temperature and its moving averages, which capture immediate and short-term impacts, while longer moving averages (7 days, 14 days) account for cumulative effects and thermal inertia, crucial for understanding stream temperature dynamics over time [11,40]. Additionally, maximum air temperature metrics help capture extreme conditions that may significantly influence stream temperatures [41]. By testing these metrics, we aim to identify the most influential air temperature predictors, improving the model's sensitivity and accuracy in forecasting post-wildfire stream temperature variations.

Table 2. Summary of explanatory variables metrics and response variables.

Explanatory Variables		
Mean_Ppt	Mean precipitation	mm
CUM1_Ppt	Antecedent cumulative precipitation over 1 day.	mm
CUM3_Ppt	Antecedent cumulative precipitation over 3 days.	mm
CUM7_Ppt	Antecedent cumulative precipitation over 7 days.	mm
CUM14_Ppt	Antecedent cumulative precipitation over 14 days.	mm
Mean_Tmean	Mean daily temperature	Celsius
MA1_Tmean	1-day moving average of the antecedent mean daily temperature	Celsius
MA3_Tmean	3-day moving average of the antecedent mean daily temperature	Celsius
MA7_Tmean	7-day moving average of the antecedent mean daily temperature	Celsius
MA14_Tmean	14-day moving average of the mean daily temperature	Celsius
7dAD_Tmean	7-day moving average daily mean air temperature	Celsius
Mean_Tmax	Mean daily maximum air temperature	Celsius
MA1_Tmax	1-day moving average of the antecedent mean daily maximum air temperature	Celsius
MA3_Tmax	3-day moving average of the antecedent mean daily maximum air temperature	Celsius
MA7_Tmax	7-day moving average of the antecedent mean daily maximum air temperature	Celsius
MA14_Tmax	14-day moving average of the antecedent mean daily maximum air temperature	Celsius
7dAD_Tmax	7-day moving average daily maximum air temperature	Celsius
Mean_Discharge	Mean stream discharge	CFS
ANT1D_Mean_Discharge	1-day antecedent mean discharge	CFS
ANT3D_Mean_Discharge	3-day antecedent mean discharge	CFS
ANT7D_Mean_Discharge	7-day antecedent mean discharge	CFS
ANT14D_Mean_Discharge	14-day antecedent mean discharge	CFS
Julian_Date	Julian Date of Calendar Year	Numerical
Pct_Burn	Percent of Watershed Area Burned	Percentage
Pct_High	Percent of Watershed Area Burned at High Severity	Percentage
Pct_Mod	Percent of Watershed Area Burned at Moderate Severity	Percentage
Pct_Low	Percent of Watershed Area Burned at Low Severity	Percentage
Response Variables		
StreamTemp_7dADM	7-day moving average daily maximum stream temperature	Celsius
Mean_Turbidity	Mean turbidity (in NTU—Nephelometric Turbidity Units)	NTU

Precipitation and discharge are critical factors influencing turbidity in streams and rivers, especially in post-wildfire scenarios [6]. To capture the variability and impacts of precipitation and discharge on turbidity, we derived several key metrics for our analysis based on historically observed daily precipitation and discharge data (Table 2). These metrics help us understand both immediate and lagged effects of precipitation and discharge on turbidity [6,42–45]. High-intensity rainfall events can lead to increased surface runoff, carrying sediment, ash, and organic debris into water bodies, significantly raising turbidity levels. Meanwhile, cumulative precipitation metrics account for delayed responses and the impact of successive rainfall events [43,46–48]. Similarly, discharge metrics capture the

erosive force of streamflow, which mobilizes sediments from the streambed and banks, elevating turbidity levels [49,50]. By incorporating these metrics, our models effectively capture the dynamic interactions between precipitation, discharge, and turbidity, enhancing our ability to predict post-wildfire water quality impacts and develop targeted management strategies [9,51]. Sensitivity analysis will be conducted to narrow down a list of the top five most influential predictors variables for each mode.

2.4. Sensitivity Analysis

To ensure the robustness and reliability of our predictive models, we employed several sensitivity analysis (SA) methods, including the Random Forest sensitivity test, Sobol sensitivity test, and Morris sensitivity test to test for variable sensitivity on our response variables—7 Day Moving Average of Daily Maximum Stream Temperature (StreamTemp_7dADM) and Mean Turbidity (Table 2). These tests are essential for understanding the influence of various parameters on the model's predictions, particularly in complex hydrologic and water quality models. The Random Forest sensitivity test uses feature importance scores to quantify the impact of each predictor variable on the model's output, helping to identify the most critical factors affecting stream temperature and turbidity in post-wildfire scenarios [52,53]. However, a key limitation of this method is that it may overlook variable interactions and can be biased toward predictors with more variability or higher cardinality. The Sobol sensitivity analysis is a method that helps explain how much each input variable and their interactions affect the variation in the model's results. This approach provides a clear and detailed understanding of which factors play the biggest roles, making it especially useful for identifying important variables in complex systems [54]. This makes it particularly useful for capturing complex, non-linear interactions among variables. However, it is computationally expensive and requires a large number of model evaluations, which can be a drawback for resource-intensive models. The Morris sensitivity test, a screening method, evaluates the effect of input variables on the model output by calculating elementary effects, which helps in identifying non-influential variables and understanding the model's response to parameter changes [55]. It is computationally less demanding compared to Sobol and can effectively filter out irrelevant predictors. However, its main limitation is that it provides less detailed information about variable interactions and may be less precise for highly complex models.

Sensitivity analysis plays a vital role in hydrologic and water quality modeling, where the interplay between spatiotemporal variability, model complexity, and parameter uncertainty demands careful evaluation. The complexity of these models, driven by the diverse interactions between climatic variables, land use, and topographic features, necessitates a thorough examination of how different parameters impact the model outcomes [56,57]. By using these sensitivity analysis methods, we can better understand the robustness of our predictions and identify key drivers of water quality changes as inputs for the machine learning models [57,58]. The top five most sensitive explanatory metrics were used to build the machine learning models. We used Random Forest (RF) and Support Vector Regression (SVR) because they effectively handle non-linear relationships and high-dimensional data, which are characteristic of post-wildfire stream temperature and turbidity dynamics. RF was chosen for its ability to capture complex interactions and provide feature importance insights, while SVR excels in modeling intricate patterns in noisy datasets. These methods strike a balance between predictive accuracy and computational efficiency, making them practical for capturing complex scenarios with minimal assumptions. A detailed study design framework is shown in Figure 2.
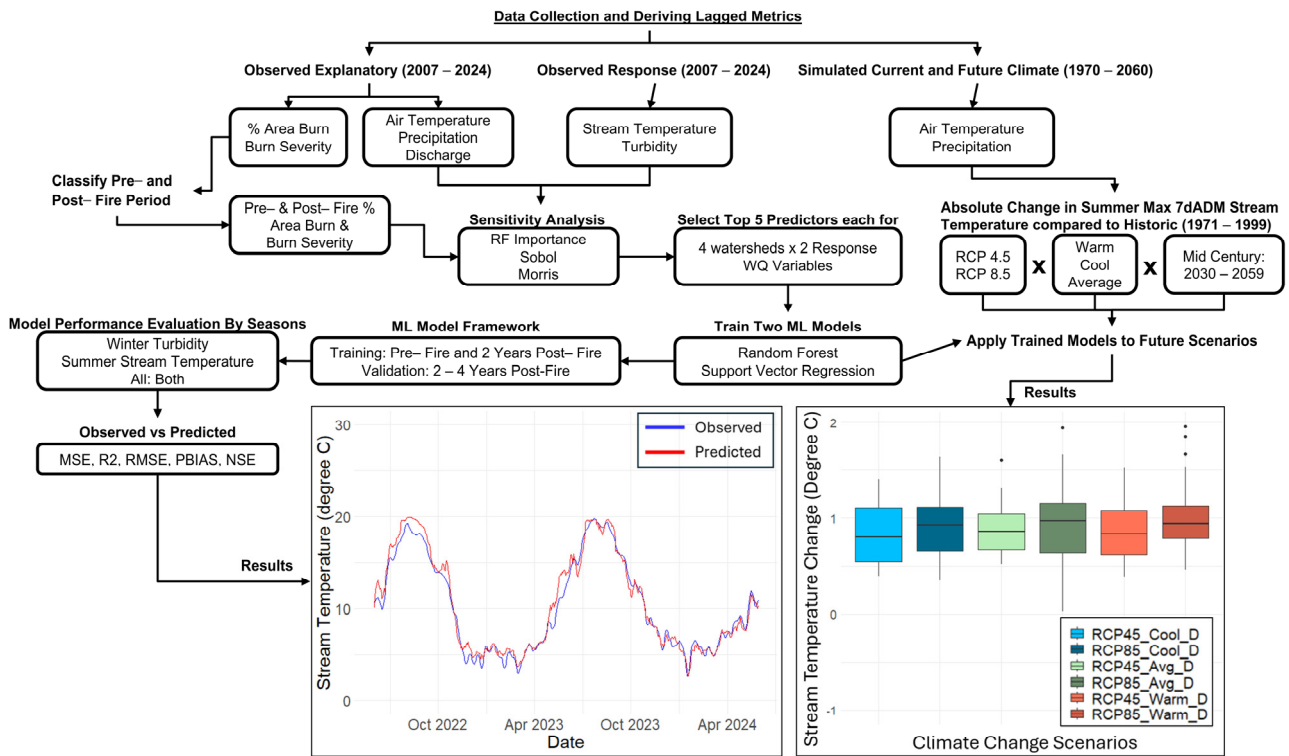
Figure 2. Research methodology conceptual framework.

2.5. Random Forest Model

In this study, the RF model was employed to predict post-wildfire stream temperature and turbidity in four burned watersheds in Oregon and Northern California. The Random Forest (RF) model combines multiple decision trees to make predictions while reducing the risk of overfitting. By averaging the outputs of individual decision trees in regression tasks, the RF model enhances prediction accuracy and reliability. This method was chosen for its ability to handle large datasets and model complex, non-linear relationships between multiple predictors and response variables. Climatic and environmental variables, such as air temperature, precipitation, and discharge, were used as input features. The RF model was trained on pre-fire data to establish a baseline and then applied to post-fire data to predict changes in stream temperature and turbidity.

Past studies have successfully utilized RF models to investigate various aspects of post-fire hydrology. For example, [59] demonstrated the effectiveness of RF models in capturing the complex interactions between fire-induced changes in land cover and subsequent hydrological responses. Similarly, [60] used RF models to predict soil erosion in post-fire environments, highlighting the model's robustness in handling diverse and complex datasets. However, gaps remain in understanding the specific impacts of climatic variables on post-fire water quality parameters such as stream temperature and turbidity. Our study addresses these gaps by analyzing feature importance scores generated by the RF model to identify the most influential variables affecting these water quality parameters in the post-wildfire environment. This approach not only enhances predictive accuracy but also improves our understanding of key drivers of water quality changes, providing crucial insights for developing targeted water management strategies and mitigating the adverse effects of wildfires on water quality [50,61].

2.6. Support Vector Regression Model

Support Vector Regression (SVR) is a powerful machine learning model designed to handle non-linear relationships and high-dimensional data by finding a hyperplane that

best fits the data while minimizing error. Several studies have utilized SVR in hydrological and environmental modeling due to its robustness. For instance, Lin et al. (2006) [62] used SVR for daily river flow predictions with high accuracy, while Asefa et al. (2006) [63] applied SVR to model reservoir inflow, effectively capturing complex non-linear relationships between variables. These examples demonstrate SVR's capability to model intricate hydrological processes, making it a suitable choice for predicting turbidity levels in post-wildfire scenarios where multiple interacting factors are present.

In water quality modeling, SVR has also shown significant effectiveness. Khan and Coulibaly (2006) [64] successfully used SVR to predict water quality indices, outperforming traditional linear models. Additionally, Yu et al. (2016) [65] applied SVR to forecast daily water temperature, effectively handling temporal dependencies and non-linearities in environmental data. These studies underscore SVR's relevance and potential in modeling turbidity in burned watersheds, where post-wildfire conditions create complex interactions between precipitation, discharge, and sediment transport. Employing SVR alongside Random Forest models leverages the strengths of both techniques, enhancing the accuracy and reliability of post-wildfire turbidity predictions.

Several studies have effectively utilized both Random Forest (RF) and Support Vector Regression (SVR) models in hydrological and environmental contexts, underscoring their complementary strengths. For instance, Abrahart et al. (2012) [66]) compared RF and SVR for river flow forecasting, finding that RF captured non-linear relationships well, while SVR excelled in handling high-dimensional data. Similarly, Chen et al. (2013) [67] applied both models to predict groundwater levels, concluding that RF was superior in terms of interpretability and robustness, whereas SVR provided higher accuracy for specific datasets. By comparing RF and SVR, these studies highlighted the distinct advantages of each method in different scenarios. RF is known for its ability to handle complex interactions and provide insights into variable importance, which is crucial for understanding the multifaceted impacts of wildfires on water quality. SVR, on the other hand, is adept at managing non-linear relationships and high-dimensional data, which are common in environmental datasets. By employing both models, we aim to leverage their respective strengths to achieve more reliable and comprehensive predictions, ultimately enhancing our understanding of post-fire water quality impacts.

2.7. Model Training, Testing, and Performance Evaluation

In this study, we built individual machine models for each watershed and response variables, we the most recent two years as testing period (2022–2024) and a combination of pre-fire and immediate post-fire years (2007–2021) as training data to evaluate the predictive performance of Random Forest (RF) and Support Vector Regression (SVR) models on stream temperature and turbidity. To capture the timing of wildfires during the training periods, we incorporated the percent watershed burn data and the percent burn at each severity level as time series data, setting pre-fire percent burn values to zero prior to the ignition date. Including post-fire data in the training period is beneficial because it allows the model to learn the changes in watershed characteristics and their impacts on streamflow, stream temperature, and turbidity due to wildfires. This inclusion helps improve the model's accuracy and robustness by enabling it to account for the effects of burn severity and extent on hydrological responses.

We employed five performance metrics to evaluate the RF and SVR models: Mean Squared Error (MSE), Coefficient of Determination (R^2), Root Mean Squared Error (RMSE), Percent Bias (PBIAS), and Nash–Sutcliffe Efficiency (NSE). These metrics provide comprehensive insights into model accuracy, bias, and overall predictive capability. MSE and RMSE measure prediction accuracy and error magnitude, while R^2 indicates the explained

variance. PBIAS assesses systematic prediction bias, and NSE evaluates the predictive power of the models. Together, these metrics offer a robust framework for understanding model strengths and limitations in predicting post-fire hydrological conditions, thereby informing resilient water management strategies [16,21,22].

2.8. Stream Temperature Projection with Downscaled Climate Models

Following performance metrics assessment of the RF and SVR models, we project stream temperature using downscaled climate models, specifically the CMIP5 downscaled MACA data [37]. To consider a range of potential future climates, we selected three models that represent warm, cool, and average air temperature scenarios (Table 3) for the mid-century period (2030 to 2059). These models were applied under two scenarios, RCP 4.5 and RCP 8.5, representing medium and high emission scenarios. We integrated the downscaled MACA data into our RF and SVR models to predict stream temperature across four distinct watersheds and compare absolute future changes with MACA-simulated historic periods (1970–1999). The projected stream temperatures were analyzed to understand the potential impacts of climate change on stream conditions. Similar approaches have been employed in previous studies. For instance, ref. [41] examined regional climate trends and their effects on stream temperature in the Pacific Northwest using downscaled climate models, while [38] studied the impacts of climate change on stream and river temperatures across the Northwest U.S. using historical climate data. To assess the changes in stream temperature, particularly the summer maximum 7-day average daily maximum (7dADM) stream temperature, we employed the t-test. This statistical test was used to compare the projected stream temperature data from 2024 to 2030 with the simulated historical data, aiming to identify significant differences in stream temperature across different climate scenarios and RCPs, thereby providing range of potential future changes in stream ecosystems.

Table 3. Summary of identified downscaled climate scenarios for each watershed.

| | **MACA Mid-Century Climate Models** | | | |
	Scenario	**RCP 4.5**	**RCP 8.5**	**Source**
Clackamas River	Warm	Can-ESM2	Can-ESM2	Canadian Centre for Climate Modelling and Analysis
	Cool	MRI-CGCM3	MRI-CGCM3	Meteorological Research Institute, Japan
	Average	GFDL-ESM2-G	GFDL-ESM2-G	Geophysical Fluid Dynamics Laboratory, USA
Russian River	Warm	Miroc-ESM-CHEM	Miroc-ESM-CHEM	Japan Agency for Marine-Earth Science and Technology
	Cool	MRI-CGCM3	MRI-CGCM3	Meteorological Research Institute, Japan
	Average	Bcc-csm1-1	Bcc-csm1-1	Beijing Climate Center, China Meteorological Administration

3. Results and Discussion

3.1. Sensitivity Analysis and Key Predictors

The sensitivity analysis for stream temperature models (Table 4 and Figure 3) revealed key variables influencing predictions across the Clackamas and Russian River Watersheds. In Clackamas River sites, MA14_Tmean and 7dAD_Tmean were the most influential variables, indicating the importance of short-term temperature averages. Julian Date also emerged as a significant predictor, underscoring seasonal impacts. For the Russian River, 7dADM_Tmean consistently ranked highest, highlighting the role of maximum temperature events. MA14_Tmean and MA7_Tmean were also important, suggesting that both short-term and longer-term temperature trends are critical [38,41,68].

For turbidity models (Table 5), Mean_Discharge was the most influential variable across all sites, emphasizing the role of streamflow in turbidity. In the Clackamas River, Mean_Ppt and cumulative precipitation (CUM1_Ppt) were significant, highlighting the impact of precipitation events. Antecedent discharge metrics (ANT1D_Mean_Discharge)

further stressed the importance of previous discharge conditions. In the Russian River, CUM1_Ppt and Mean_Ppt were similarly important, with antecedent discharge metrics (ANT14D_Mean_Discharge and ANT7D_Mean_Discharge) underscoring the role of historical discharge patterns [6,45].

Table 4. Stream temperature sensitivity analysis results with top five most impactful metrics.

	Stream Temperature Model Sensitivity			
	Clackamas River		Russian River	
Rank	14211010 Estacada	14210000 Oregon City	11462500 Hopland	11467000 Guerneville
1st	MA14_Tmean	MA14_Tmean	7dADM_Tmean	7dADM_Tmean
2nd	Julian Date	7dAD_Tmean	Julian Date	MA14_Tmean
3rd	MA7_Tmean	Julian Date	MA14_Tmean	Julian Date
4th	7dADM_Tmean	MA14_Tmax	7dADM_Tmax	7dADM_Tmax
5th	7dADM_Tmax	MA7_Tmean	MA7_Tmean	MA7_Tmean

Table 5. Turbidity sensitivity analysis results with top five most impactful metrics.

	Turbidity Model Sensitivity			
	Clackamas River		Russian River	
Rank	14211010 Estacada	14210000 Oregon City	11462500 Hopland	11467000 Guerneville
1st	Mean_Discharge	Mean_Discharge	Mean_Discharge	Mean_Discharge
2nd	ANT1D_Mean_Discharge	Mean_Ppt	CUM1_Ppt	Mean_Ppt
3rd	CUM1_Ppt	CUM1_Ppt	Mean_Ppt	CUM1_Ppt
4th	CUM3_Ppt	Julian Date	ANT14D_Mean_Discharge	ANT14D_Mean_Discharge
5th	Julian Date	ANT1D_Mean_Discharge	ANT7D_Mean_Discharge	ANT7D_Mean_Discharge
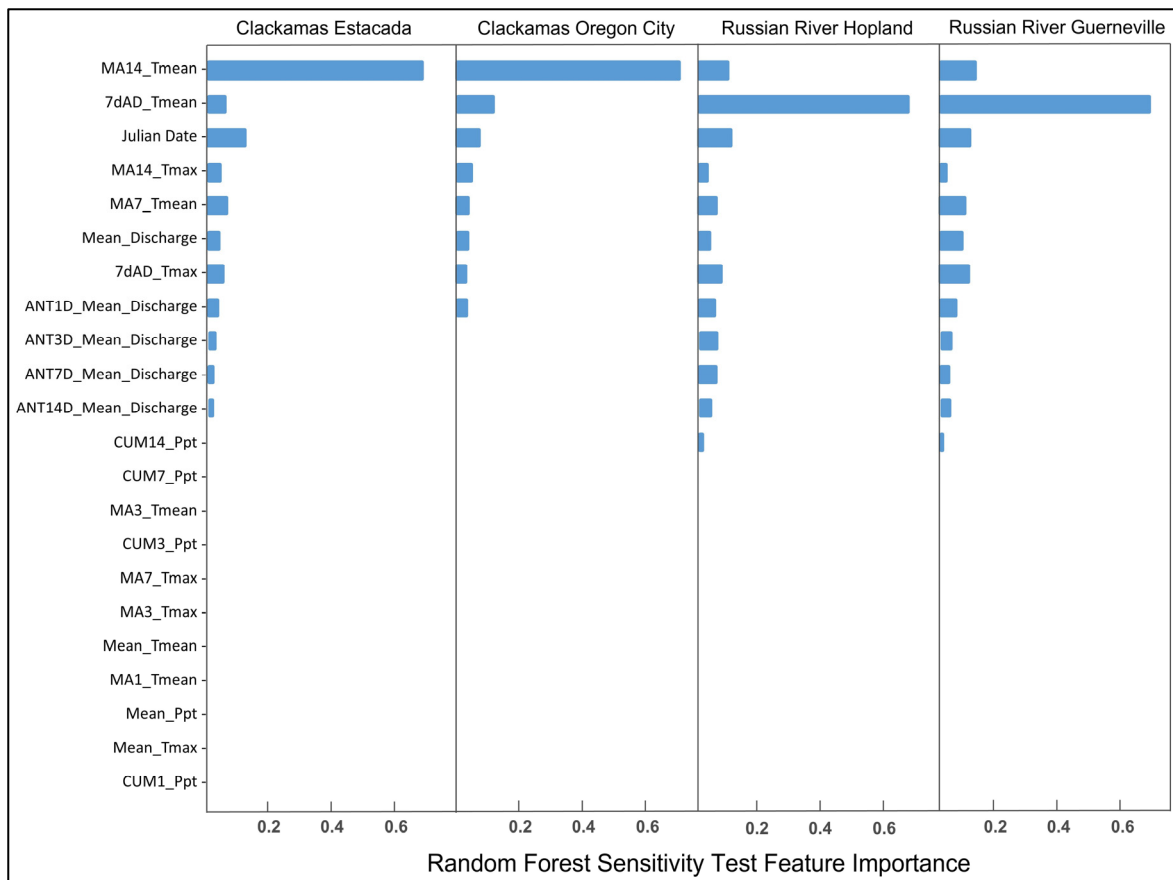
Figure 3. Bar graphs showing random forest sensitivity test feature importance of explanatory variables for 7dADM stream temperature as response variables in four study watersheds.

For both stream temperature and turbidity, the percent watershed burned and percent burned at each severity level were not significant predictors and did not have major impacts on model sensitivity. This result can be attributed to the fact that all four of our studied watersheds burned less than or equal to 20% of the watershed area in each fire event (Table 1). This finding is also consistent with prior research results where significant hydrological responses may be absent in watersheds with less than 20% area burned [35,69,70]. These results emphasize that the extent of watershed burning plays a crucial role in determining hydrological impacts and highlights the importance of incorporating both climatic and hydrological factors in stream temperature and turbidity models for accurate predictions and effective water resource management in the context of climate change.

Less important variables that did not significantly influence model outcomes were excluded from the final model inputs. This decision was guided by the results of the sensitivity analysis, which highlighted the key predictors driving the model's performance. By excluding these less influential variables, the models were streamlined to focus on the most relevant variables, reducing the potential for overfitting and improving overall model accuracy. Notably, the Random Forest and Support Vector Regression models used in this study are less impacted by multicollinearity compared to traditional regression models [71,72]. This inherent robustness allows these machine learning methods to handle correlated variables more effectively, further supporting the decision to prioritize key variables while excluding those with minimal impact.

### 3.2. Stream Temperature Model Performance

3.2.1. Clackamas River Watershed

The results, shown in Figures 4 and 5 and Table 6, highlight the models' accuracy during the entire testing period (ALL) and the summer months (June–September). At the Clackamas River at Estacada, The RF model generally outperforms the SVR model, particularly when considering the entire dataset, with higher R^2 (0.98 vs. 0.97) and lower RMSE (0.88 vs. 1.09), indicating better overall explanatory power and more accurate predictions. However, during the summer months, both models perform similarly, with identical MSE and NSE values, indicating comparable capability in capturing seasonal variations. The higher MSE and RMSE values in summer suggest greater variability and challenges in accurate prediction during this period. The increased PBIAS (3.20) for summer models indicate a systematic overestimation of stream temperature, likely due to elevated temperatures and reduced flow rates, amplifying prediction errors. At the Clackamas River in Oregon City, both RF and SVR models show high predictive accuracy, with R^2 values close to 0.97 for the all-season models. However, during the summer, the predictive power decreases, particularly for the RF model, which drops to an R^2 of 0.85. Despite this, the summer-specific SVR model maintains relatively high accuracy, demonstrating its robustness across different seasons.

Reservoirs in the Clackamas River basin, including those managed by Portland General Electric, play a significant role in moderating downstream water temperatures. These reservoirs release cooler water from their lower depths during summer, which can help mitigate temperature spikes. At Estacada, forest land cover is higher and the Riverside Fire in 2020 burned 20% of the watershed (Table 1), which may have reduced canopy cover and increased solar radiation reaching the river, leading to higher summer temperatures and greater prediction challenges for the models. The combination of natural and fire-induced changes in canopy cover and shading likely influences the summer temperature dynamics and the higher MSE and RMSE values observed. In contrast, Oregon City, located further downstream, benefits more from the moderating effects of upstream reservoirs.
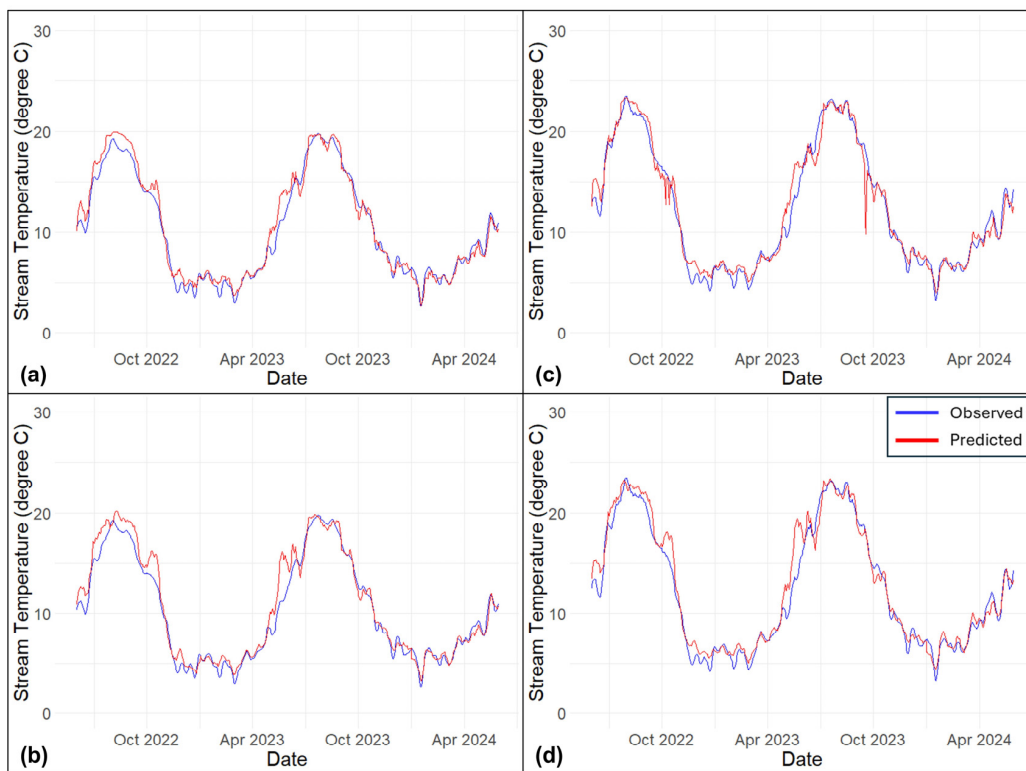
Figure 4. Observed versus Predicted 7dADM stream temperature time series for (**a**) Estacada RF, (**b**) Estacada SVR, (**c**) Oregon City RF, and (**d**) Oregon City SVR in the Clackamas River Watersheds over the post-fire testing period.
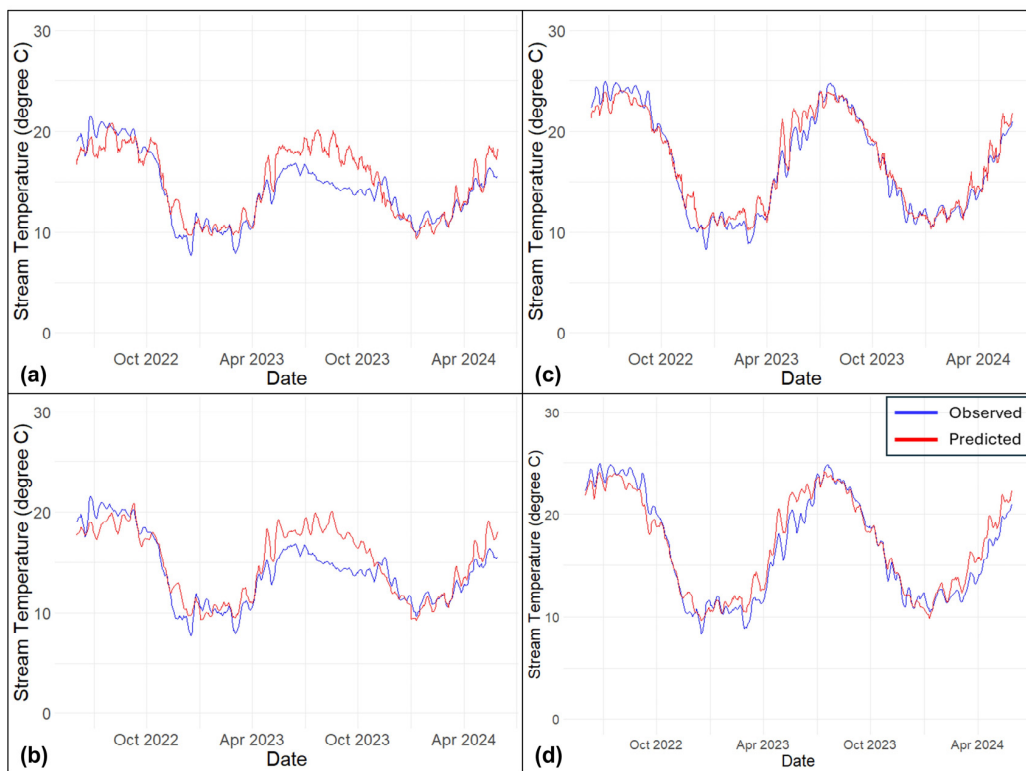
Figure 5. Comparison between observed and predicted 7dADM stream temperature time series for (**a**) Hopland RF, (**b**) Hopland SVR, (**c**) Guerneville RF, and (**d**) Guerneville SVR in the Russian River Watersheds over the post-fire testing period.

Table 6. Stream temperature RF and SVR model performance summary.

Stream Temperature	MSE	R^2	RMSE	PBIAS	NSE
14210000 Clackamas River at Estacada					
RF_All	0.77	0.98	0.88	3.20	0.97
RF_Summer	0.96	0.90	0.98	3.20	0.86
SVR_All	1.19	0.97	1.09	4.90	0.95
SVR_Summer	1.29	0.88	1.13	4.30	0.81
14211010 Clackamas River at Oregon City					
RF_All	1.12	0.97	1.06	1.40	0.97
RF_Summer	1.50	0.85	1.22	0.00	0.83
SVR_All	1.41	0.97	1.19	3.80	0.96
SVR_Summer	1.14	0.89	1.07	1.90	0.87
11462500 Russian River at Hopland					
RF_All	3.38	0.77	1.84	5.20	0.70
RF_Summer	6.37	0.09	2.52	5.40	−0.07
SVR_All	3.36	0.77	1.83	5.50	0.70
SVR_Summer	5.94	0.11	2.44	4.60	0.00
11467000 Russian River at Guerneville					
RF_All	1.02	0.97	1.01	1.70	0.96
RF_Summer	0.92	0.74	0.96	−1.40	0.69
SVR_All	1.49	0.95	1.22	2.30	0.94
SVR_Summer	1.28	0.65	1.13	−1.90	0.56

3.2.2. Russian River Watershed

For the Russian River at Hopland, both the RF and SVR models exhibit moderate predictive accuracy for the all-season models, but performance drastically decreases during the summer. The RF summer model shows a near-zero R^2, indicating a poor fit, and a negative NSE value, suggesting that the model predictions are less accurate than simply using the mean of the observed data. The SVR summer model also shows significantly reduced performance, highlighting the challenges in modeling stream temperatures in this region during summer. The Russian River at Guerneville displays a contrasting pattern where the all-season RF and SVR models perform exceptionally well with an R^2 of 0.97 and 0.95. However, during the summer, both the RF and SVR models experience a drop in predictive power, although the decline is more pronounced in the SVR model. The RF summer model maintains a decent R^2 of 0.74, while the SVR summer model falls to 0.65, indicating that RF models may be more resilient in certain conditions.

Several factors could explain these performance discrepancies between Hopland and Guerneville. Firstly, the difference in drainage area might play a role (Table 1). Guerneville's larger drainage area (3465 km^2) compared to Hopland's (938 km^2) could lead to more stable stream temperature patterns, making it easier for models to predict accurately. Additionally, the percentage of watershed burned is higher at Hopland (18%) than at Guerneville (13%), potentially causing more significant disruptions in stream temperature due to increased erosion, sediment transport, and altered hydrology. Furthermore, land cover differences might also impact model performance. The percentage of forest cover at Hopland is considerably lower (29.8%) compared to Guerneville (32.4%), while the percentage of shrub/grassland is higher at Hopland (57.2% versus 47.6%). This difference in vegetation cover could affect microclimatic conditions and hydrological responses, influencing stream temperature patterns and making them more complex to predict at Hopland.

3.2.3. Comparison Between Clackamas and Russian River Watersheds

The particularly poor performance of both models at the Hopland site during the summer months, as illustrated in Figure 5, where the models consistently underpredict stream temperatures until September 2022, can be attributed to the significant hydrological impacts of recent wildfires and prolonged drought years [73]. Post-fire conditions often result in increased solar radiation due to the loss of riparian vegetation, higher sediment loads, and altered streamflow patterns, all of which can exacerbate temperature fluctuations. This phenomenon is supported by research indicating that wildfire can lead to reduced

canopy cover and changes in streambed composition, which collectively increase water temperatures [44,74].

These post-fire effects are likely more pronounced in the Russian River watershed due to its unique climatic and land cover characteristics, such as more agricultural lands and shrubs instead of forests (Table 1) and more frequent droughts that hinder the moisture needed for vegetation recovery [75]. Interestingly, both RF and SVR models overpredicted stream temperatures during the summer of 2023, which can be expected due to the back-to-back atmospheric rivers hitting Northern California in the winter of 2022, alleviating the multi-year drought and encouraging vegetation growth that lowers stream temperatures [76]. Since both RF and SVR models do not include streamflow as a predictor, the overprediction may also be attributed to the increase in summer reservoir releases from Lake Sonoma and Lake Mendocino, which were both filled during the heavy winter storms.

On the other hand, the Clackamas River's more stable and forested environment provides a conducive setting for more accurate and reliable stream temperature predictions. The Russian River's variable climate and recent wildfire disturbances pose challenges for predictive models. These results suggest that while both RF and SVR models have their strengths, the RF model outperformed the SVR model in this context likely due to its robustness in handling complex interactions and non-linear relationships in the stream temperature data across different watersheds and seasonal variations. However, water management practices such as summer reservoir releases in both the Clackamas River and Russian River may introduce complications in RF and SVR modeling.

The high level of statistical significance in our results can be attributed to the careful selection of predictor variables and the rigorous application of sensitivity analysis methods. While the significance might seem high, it reflects the robustness of the models in capturing the critical factors influencing stream temperature and turbidity. Moreover, both RF and SVR models are designed to handle complex, non-linear relationships, reducing the likelihood of spurious correlations, and they are less affected by multicollinearity, allowing them to focus on identifying the most influential predictors without being skewed by correlations among variables. The significance is, therefore, a result of these models' capacity to effectively discern meaningful patterns in the data rather than an artifact of the sampling process.

3.3. Turbidity Model Performance

3.3.1. Clackamas River Watershed

The RF and SVR models for turbidity prediction at various sites present some intriguing findings (Table 7). At the Clackamas River at Estacada, the across all-season RF model shows better performance metrics than its SVR counterpart. Interestingly, both winter-specific models (RF and SVR) show identical performance, indicating that winter conditions might affect model predictions uniformly. Winter months typically have precipitation patterns that allow for more consistent turbidity behavior, including increased precipitation and runoff, which directly influence turbidity levels. These consistent patterns can make it easier for the model to capture and predict changes in turbidity accurately. Additionally, winter conditions may lead to more consistent sediment transport and deposition processes via increased flow in the river, reducing variability in turbidity readings. During winter, the river is less likely to experience sporadic disturbances that can occur during other seasons (Figure 6), such as sudden storms or dry spells, which can introduce noise and make it harder for sediment to mobilize and be transported downstream.
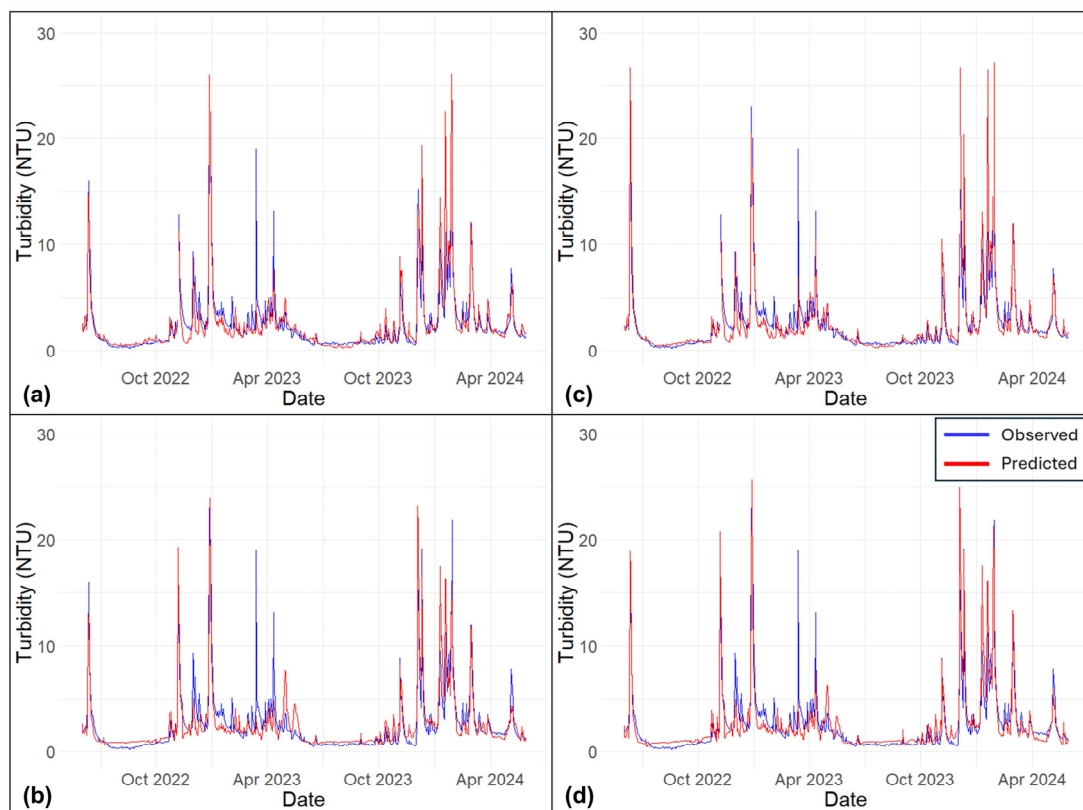
Figure 6. Comparison between observed and predicted turbidity time series for (**a**) Estacada RF, (**b**) Estacada SVR, (**c**) Oregon City RF, and (**d**) Oregon City SVR in the Clackamas River Watersheds over the post-fire testing period.

At the Clackamas River in Oregon City, both RF and SVR models exhibit strong predictive power with high R^2 values, especially during all seasons. However, during winter, the predictive accuracy drops slightly, with both RF and SVR models showing higher errors and biases. Oregon City may have more urbanized areas contributing to runoff, leading to more variable and less predictable turbidity levels. Urban runoff can carry diverse pollutants and sediments, making it harder for the model to capture the relationships accurately. This finding suggests that winter conditions introduce complexities in turbidity prediction due to differences between the more natural upstream areas and the downstream urban areas. These complexities arise from variations in lag time between precipitation and peak turbidity, as well as the hysteresis behavior of the hydrograph, both of which are influenced by differing levels of impervious surfaces [47].

Table 7. Turbidity RF and SVR model performance summary.

Turbidity	MSE	R^2	RMSE	PBIAS	NSE
14210000 Clackamas River at Estacada					
RF_All	3.39	0.84	1.84	1.10	0.80
RF_Winter	6.76	0.89	2.60	3.60	0.80
SVR_All	4.83	0.74	2.20	−5.60	0.71
SVR_winter	6.76	0.89	2.60	3.60	0.80
14211010 Clackamas River at Oregon City					
RF_All	3.14	0.87	1.77	1.10	0.81
RF_Winter	7.89	0.87	2.81	2.30	0.77
SVR_All	3.65	0.80	1.91	−5.40	0.78
SVR_winter	7.89	0.87	2.81	2.30	0.77

Table 7. *Cont.*

| Turbidity	MSE	R^2	RMSE	PBIAS	NSE
11462500 Russian River at Hopland					
RF_All	291.54	0.87	17.07	3.80	0.76
RF_Winter	710.22	0.88	26.65	19.90	0.71
SVR_All	243.11	0.81	15.59	−10.40	0.80
SVR_winter	710.22	0.88	26.65	19.90	0.71
11467000 Russian River at Guerneville					
RF_All	218.30	0.89	14.78	14.20	0.83
RF_Winter	506.21	0.86	22.50	14.70	0.79
SVR_All	448.50	0.70	21.18	14.40	0.66
SVR_winter	986.98	0.64	31.42	11.10	0.60

3.3.2. Russian River Watershed

For the Russian River at Hopland, the models show a stark contrast in performance. Both RF and SVR models exhibit significantly higher errors and biases, especially during winter. The extremely high MSE and RMSE values for the RF Winter and SVR Winter models suggest that these models struggle considerably with turbidity prediction in winter. This could be attributed to unique watershed characteristics due to the majority of the watershed being dominated by shrubs and grasslands, creating a non-linear response in turbidity levels that introduce substantial variability, which the models fail to predict accurately.

The Russian River at Guerneville presents a different scenario where the all-season RF model performs exceptionally well, similar to the Clackamas River sites. However, the winter-specific models show a marked decrease in performance in Guerneville, particularly the SVR Winter model. The substantial drop in R^2 and increase in error metrics highlight that SVR models may be less resilient to seasonal variations compared to RF models. This emphasizes the need for incorporating additional environmental and climatic variables to improve model robustness, especially during challenging winter conditions.

3.3.3. Comparison Between Clackamas and Russian River Watersheds

The Russian River site tends to underpredict turbidity (Figure 7) more while the Clackamas River sites follow observation pretty well, likely due to differences in watershed characteristics. The smaller, nested watershed may experience more pronounced hydrological responses to rainfall and post-fire conditions, leading to higher sediment transport and turbidity. Conversely, the larger Guerneville Watershed might buffer these effects due to a lower percentage of watershed burned, resulting in under-predictions. Wildfire impacts, including increased erosion and sediment loads [7], can exacerbate these differences, as smaller watersheds are more sensitive to such disturbances [23].

The reduction in accuracy during winter months for Guerneville could be attributed to impacts from cumulative and multiples wildfires impacts such as increased sediment loads due to the loss of vegetation and changes in soil stability, which can exacerbate turbidity fluctuations [1]. This phenomenon is supported by research indicating that wildfire can lead to increased erosion, higher sediment transport [77], and altered streamflow patterns, all of which contribute to higher turbidity [45,78]. These post-fire effects are likely more pronounced in the Russian River watershed due to its unique Mediterranean climate and lower summer flows due to lack of precipitation in late spring, as well as the presence of numerous reservoirs that can buffer sediment impacts but also complicate hydrological responses. The Clackamas River Watershed on the other hand, exhibits more stable streamflow throughout the year from consistent rainfall, and heavily forested area with a high infiltration rate help in reducing runoff and sediment transport. Current dams along the Clackamas River Watershed further capture sediment and regulate stream temperatures, making the watershed more resilient to the hydrological impacts of wildfires downstream.
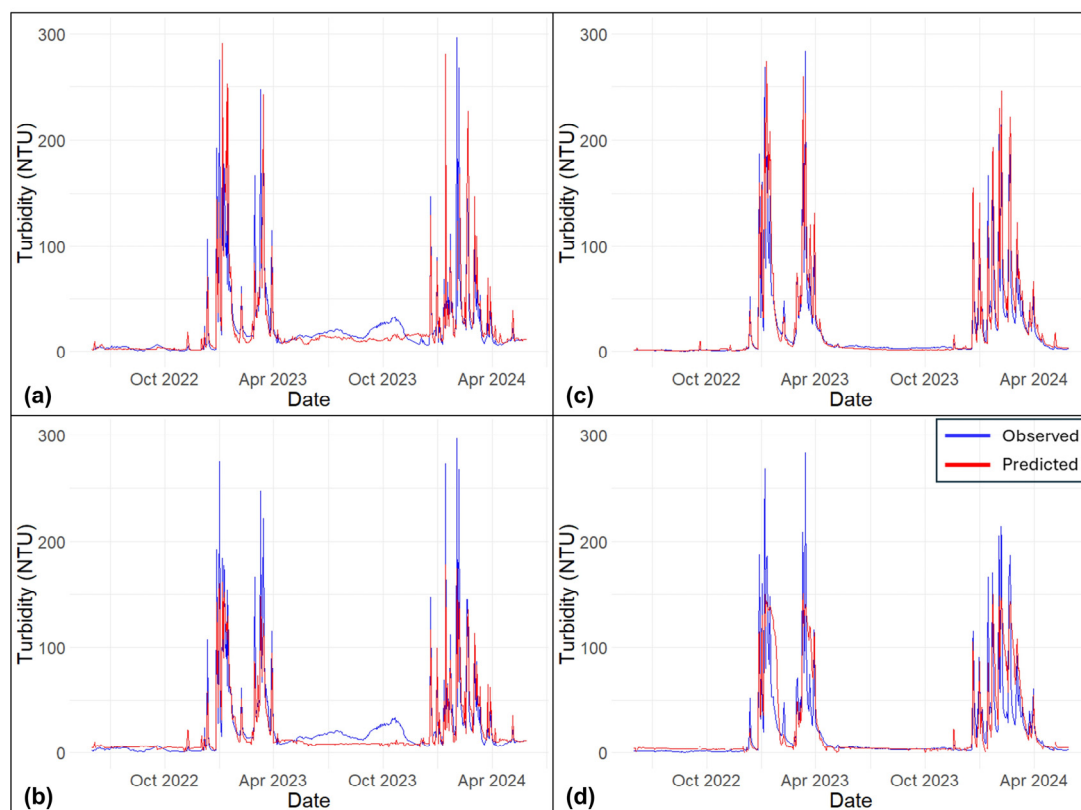
Figure 7. Comparison between observed and predicted turbidity time series for (**a**) Hopland RF, (**b**) Hopland SVR, (**c**) Guerneville RF, and (**d**) Guerneville SVR in the Russian River Watersheds over the post-fire testing period.

The discrepancies in model performance, such as overprediction and underprediction, across the Clackamas and Russian River Watersheds can be attributed to the distinct hydrological and geomorphological characteristics of each watershed. In the Russian River Watershed, the under-prediction of turbidity may be linked to its Mediterranean climate, where low summer flows and post-wildfire conditions can create complex sediment transport dynamics that are difficult for models to accurately capture. The presence of reservoirs, which can buffer sediment but also alter streamflow patterns, adds another layer of complexity that might contribute to the models' struggle in predicting turbidity during winter months.

Conversely, the Clackamas River Watershed, with its more consistent rainfall and stable streamflow throughout the year, offers a more predictable environment for sediment transport, leading to better model performance. The high infiltration rates in its heavily forested areas reduce surface runoff and sediment transport, which, coupled with the sediment capture by dams, results in a system less prone to the extremes that complicate turbidity prediction in more variable watersheds like the Russian River. These differences highlight the importance of considering watershed-specific factors when interpreting model performance, as the unique interactions between climate, land use, and hydrological processes can lead to varying levels of prediction accuracy.

### 3.4. Simulated Future Stream Temperature

3.4.1. Clackamas River Watershed

The analysis of projected future versus historic stream temperatures at both sites in the Clackamas River under RCP 4.5 and RCP 8.5 scenarios (Table 3) indicates significant warming across all future climate conditions (cool, average, and warm). As shown in

Table 8 and Figures 8 and 9, both RF and SVR models predict considerable increases of up to 2.2 degrees Celsius in summer 7dADM stream temperatures for the period 2030–2059 compared to 1970–1999. The RF models generally show higher sensitivity to climate change, indicated by larger t-values, suggesting more pronounced differences from historical temperatures. These results highlight that under moderate (RCP 4.5) and extreme (RCP 8.5) climate scenarios, stream temperatures are projected to rise significantly, impacting cool (+0.43~2.05 °C), average (+0.55~2.18 °C), and warm (+0.7~2.22 °C) scenarios (Figure 8).

Table 8. T-test results showing t-value and significance between modeled future and historic stream temperature. *** indicates $p < 0.001$ level of significance; ** indicates $p < 0.01$ level of significance.

Historic: 1970–1999 Future: 2030–2059	Clackamas River				Russian River			
	Estacada		Oregon City		Hopland		Guerneville	
	RF	SVR	RF	SVR	RF	SVR	RF	SVR
RCP4.5_Cool vs. Hist_Cool	26.46 ***	17.58 ***	10.22 ***	4.35 ***	13.01 ***	22.07 ***	3.18 ***	14.16 ***
RCP8.5_Cool vs. Hist_Cool	26.78 ***	18.27 ***	10.92 ***	3.91 ***	13.79 ***	20.82 ***	4.62 **	16.80 ***
RCP4.5_Avg vs. Hist_Avg	18.49 **	14.44 ***	9.24 ***	4.12 ***	12.90 ***	22.20 ***	5.08 **	13.40 ***
RCP8.5_Avg vs. Hist_Avg	18.63 ***	14.76 ***	9.41 ***	4.62 ***	15.23 ***	26.94 ***	4.47 ***	13.81 ***
RCP4.5_Warm vs. Hist_Warm	21.89 ***	17.53 ***	11.16 ***	7.71 ***	15.42 ***	17.71 ***	4.06 ***	10.64 ***
RCP8.5_Warm vs. Hist_Warm	22.12 ***	17.31 ***	11.48 ***	6.99 ***	12.69 ***	22.72 ***	3.19 ***	13.50 ***
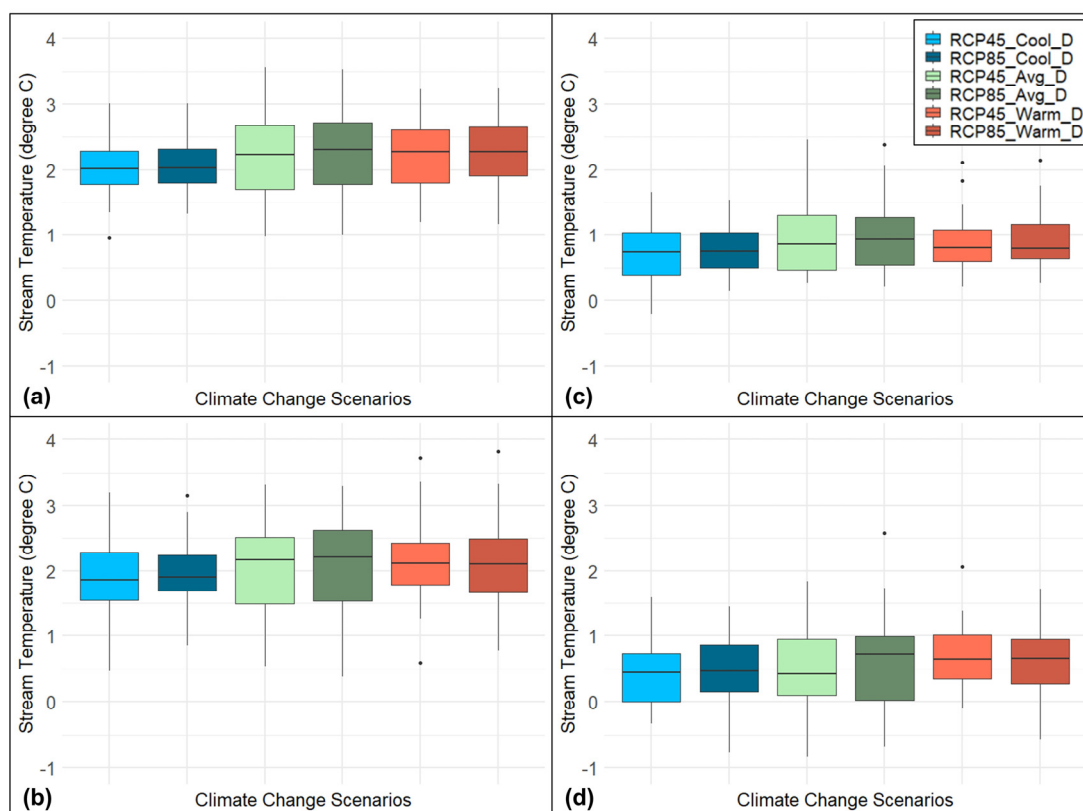
Figure 8. Change in summer max 7dADM stream temperature under future (2030–2059) climate projections compared to historical (1970–1999) for (**a**) Estacada RF, (**b**) Estacada SVR, (**c**) Oregon City RF, and (**d**) Oregon City SVR in the Clackamas River Watersheds.
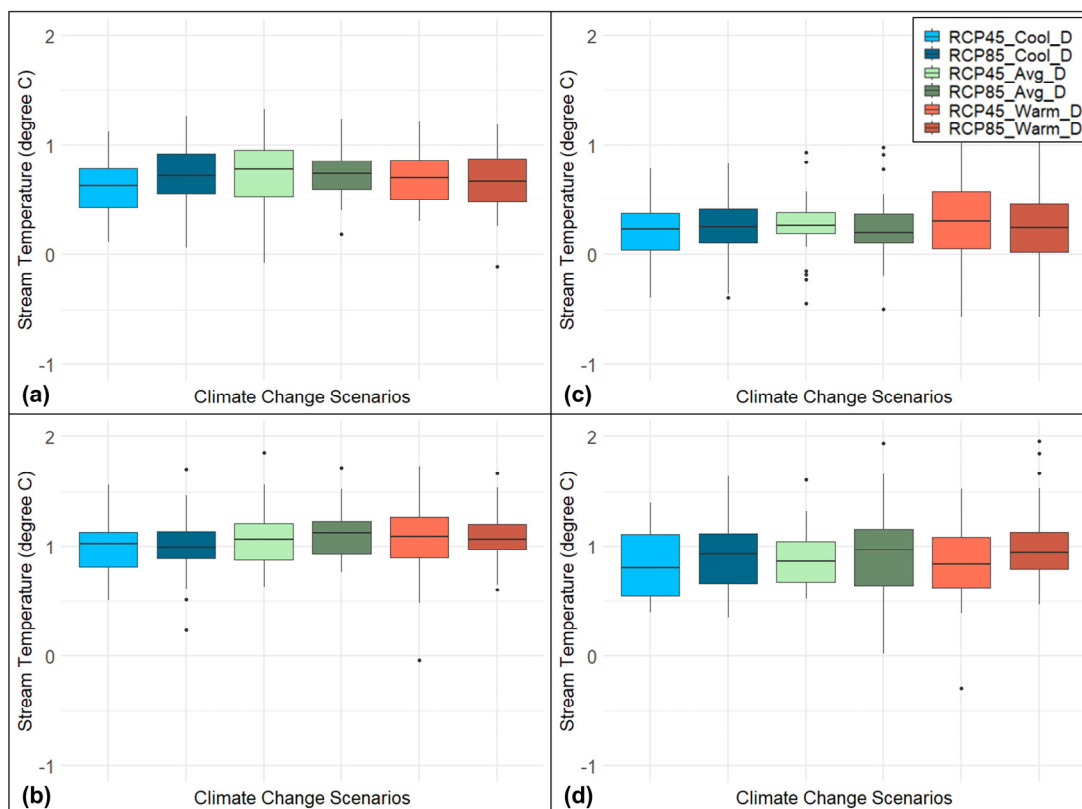
Figure 9. Change in summer max 7dADM stream temperature under future (2030–2059) climate projections compared to historical (1970–1999) for (**a**) Hopland RF, (**b**) Hopland SVR, (**c**) Guerneville RF, and (**d**) Guerneville SVR in the Russian River Watersheds.

This finding indicates that extreme warming is anticipated under future climate conditions, especially during warm periods, potentially exacerbating stress on aquatic ecosystems. These findings indicate that without intervention, future climate conditions will likely lead to significant warming of stream temperatures in the Clackamas River Watershed. The consistent upward shift in temperatures across all scenarios, as highlighted in the box plots, underscores the urgency for adaptive water management strategies to mitigate the impacts of climate change and to address the anticipated significant warming of stream temperatures and its effects on water quality and ecosystem health.

3.4.2. Russian River Watershed

For the Hopland location, the RF model projections indicate a general increase in summer maximum 7dADM stream temperatures across all climate change scenarios. The median values for each scenario show a consistent warming trend, with the RCP8.5_Warm_D scenario exhibiting the largest increase. The range of projected changes is wider under the RCP8.5 scenarios, indicating greater uncertainty in high emission scenarios. The SVR model projections for Hopland also show an increase in stream temperatures, but with a slightly different pattern compared to the RF model. The SVR model indicates a more pronounced increase under the RCP4.5_Warm_D scenario compared to the RF model, while the RCP8.5 scenarios show a similar range of projected changes as observed in the RF model. The differences between the RF and SVR model projections highlight the variability in model responses to climate change scenarios.

For the Hopland location, both RF and SVR models indicate a general increase in summer maximum 7dADM stream temperatures across all climate change scenarios, with the RCP8.5_Warm_D scenario exhibiting the largest increase. The RF model shows a

broader range of projected changes compared to the SVR model, especially under the high emission scenario RCP 8.5, indicating greater uncertainty. At the Guerneville location, the RF and SVR models also project increases in stream temperatures for all scenarios, but with a slightly lower magnitude compared to Hopland. The RCP8.5_Warm_D scenario again shows the highest increase, with a noticeable spread in the range of projections. The variability among the different scenarios is less pronounced at Guerneville, indicating a more consistent response to climate change.

The projected increases in summer maximum 7dADM stream temperatures for the Russian River at both Hopland and Guerneville indicate a significant impact of climate change on stream thermal regimes. However, the magnitude of change and variability differ between the two sites. Hopland shows a higher increase in stream temperatures compared to Guerneville, particularly under the high emission scenario RCP 8.5. This could be due to local factors such as watershed characteristics, land use, and microclimate conditions that influence stream temperatures. The wider range of projections at Hopland suggests higher sensitivity to climate change impacts in this region. The significant t-test values for Hopland (ranging from 12.69 to 26.94) reflect a strong response to climate change scenarios. The differences observed between the RF and SVR model projections underscore the importance of using multiple modeling approaches to capture the range of potential future conditions. The RF model tends to show a broader range of projected changes, especially under the high emission scenario RCP 8.5, reflecting the model's sensitivity to extreme conditions. The SVR model shows a narrower range of projected changes, indicating less variability in its projections.

3.4.3. Comparison Between Clackamas and Russian River Watershed

In both watersheds, the RCP8.5 scenarios consistently show higher increases in stream temperatures compared to RCP4.5, reflecting the higher greenhouse gas concentrations and associated warming under the RCP8.5 pathway. This indicates that the extent of future warming and its impact on stream temperatures will be significantly influenced by the trajectory of greenhouse gas emissions. The wider range of projections under RCP8.5 also suggests greater uncertainty and variability in future climate conditions, underscoring the importance of mitigation efforts to limit greenhouse gas emissions and reduce climate change impacts.

The context of wildfire impacts on stream temperatures is crucial. Post-fire conditions can exacerbate stream temperature increases due to reduced canopy cover and altered hydrology, leading to higher solar radiation exposure and decreased shade [78–80]. These changes can be more pronounced in smaller watersheds like Estacada and Hopland, where the effects of wildfires are more concentrated and less mitigated by landscape diversity. Conversely, larger watersheds like Oregon City and Guerneville might experience a more moderated impact due to their extensive buffering capacity. The differences in prediction range between RF and SVR models indicate that while RF generally captures broader trends, SVR might be more sensitive to specific climate scenarios, highlighting the importance of using multiple modeling approaches to understand future stream temperature dynamics.

3.5. Uncertainties and Study Limitations

Uncertainties within downscaled climate models and assumptions inherent in the RF and SVR models introduce additional complexity to these predictions. Downscaled models, despite their utility, are limited by the accuracy of their input data and the assumptions regarding future climatic conditions [81,82]. Moreover, the RF and SVR models' performance in capturing future stream temperatures can be inconsistent, particularly in

areas with complex hydrological responses to climatic changes, such as Hopland. This inconsistency can lead to an underestimation or overestimation of future temperatures and subsequently impact water quality predictions [83,84]. Therefore, these results should be interpreted with caution, considering the inherent uncertainties in climate projections and model assumptions.

While our study advances the understanding of post-wildfire water quality dynamics, several limitations should be acknowledged. Model uncertainties arise because the accuracy of RF and SVR models is inherently dependent on the quality and quantity of input data. Incomplete or biased data can lead to inaccurate predictions. This is particularly relevant in the Hopland site, where poor model performance was noted, highlighting the challenges in capturing complex hydrological responses [81,82]. Downscaled climate models, while useful for localized predictions, come with inherent uncertainties due to the assumptions and input data limitations [83,84]. These uncertainties can compound the prediction errors in stream temperature and turbidity. The spatial and temporal extent limitations of our study are evident, as it focuses on specific watersheds with unique geographical and climatic conditions. Extrapolating these findings to other regions may not be straightforward due to the variability in watershed characteristics and wildfire impacts. Additionally, to better address the temporal effects of watershed vegetation recovery, future research can consider incorporating variables that change over time, such as the Normalized Difference Vegetation Index (NDVI), Leaf Area Index (LAI), biomass, and time since burning.

A key limitation of this study is the geographic and hydrological specificity of the selected watersheds. The Clackamas and Russian River watersheds differ in size, land cover, and climatic conditions, which limits the generalizability of the findings to other regions with varying watershed characteristics. For example, the Clackamas River watershed benefits from consistent forest cover and rainfall patterns that stabilize baseflows, while the Russian River watershed is influenced by a Mediterranean climate and variable water management operations. The relatively small size of some subwatersheds, such as Hopland, may lead to more pronounced post-fire hydrological responses that complicate model predictions. Expanding the study to include additional watersheds could help identify broader trends and improve predictive model robustness. Additionally, capturing long-term post-fire recovery processes, such as changes in vegetation regrowth, is essential for understanding sustained impacts on water quality.

In this study, while the idea of developing a regional model using machine learning approaches like Random Forest and Support Vector Regression is appealing for its potential to generalize across multiple watersheds, our findings suggest that these models are more effective when tailored to individual watersheds due to their hyper-specialized nature. The variability between watersheds—such as differences in land cover, burn severity, and hydrological responses—makes it challenging for a regional model to achieve the same level of precision as a watershed-specific model. Additionally, although RF and SVR are robust against multicollinearity, we observed that highly correlated variables can still appear significant in a hyper fitted model without necessarily improving predictive performance [21,85]. This underscores the importance of careful variable selection and the need to avoid overfitting, ensuring that models remain both accurate and generalizable. Ultimately, while regional models may offer broad insights, the most reliable predictions in this context are achieved through models that are finely tuned to the specific characteristics of each watershed.

3.6. Implications for Water Resource Management and Recommendations

Water reservoir operations play a critical role in regulating stream temperatures [86] in both the Clackamas and Russian River Watersheds, particularly during the dry summer months when natural baseflows are insufficient to mitigate rising stream temperatures. In the Clackamas River, reservoirs managed by Portland General Electric release cooler water from deeper reservoir layers, helping to offset post-wildfire warming effects and stabilize stream temperatures downstream, which supports coldwater species such as salmonids. In contrast, reservoirs in the Russian River Watershed, such as Lake Mendocino and Lake Sonoma, augment summer flows but may still result in elevated downstream temperatures due to prolonged surface exposure and ambient air temperatures.

Future climate projections indicate more frequent droughts, higher air temperatures, and increased variability in precipitation [87], which will likely require reservoir operators to balance competing priorities more intensely, such as conserving storage for extended dry seasons versus maintaining sufficient downstream releases for ecological needs. These changes could reduce the ability to mitigate extreme temperature spikes unless operations incorporate more flexible, adaptive strategies, such as dynamic release schedules, coordinated inter-basin transfers, and increased use of predictive climate models. The relevance of our results lies in demonstrating that while current reservoir operations help buffer post-wildfire impacts on stream temperatures. Future conditions may challenge this buffering capacity, necessitating proactive adjustments to avoid further stressing aquatic ecosystems, particularly in drought-prone watersheds like the Russian River.

The findings of this study underscore the critical role of machine learning models in predicting post-wildfire stream temperature and turbidity, with Random Forest (RF) models demonstrating superior performance in capturing complex non-linear interactions between climatic variables and hydrological responses. Key predictors, such as the 14-day moving average of air temperature (MA14_Tmean) and mean discharge, were identified as significant drivers of post-fire water quality changes, providing valuable insights for improving water quality forecasting. While the results are specific to the Clackamas and Russian River Watersheds, the framework developed in this study can be adapted for other wildfire-prone watersheds with similar climatic and hydrological challenges. Expanding this approach to additional watersheds with diverse geological and land use characteristics can help evaluate the generalizability of the models and inform broader regional water management strategies.

Future research should incorporate dynamic variables such as vegetation recovery indices (e.g., NDVI, LAI) and soil moisture to improve long-term post-fire predictions, particularly for smaller watersheds where recovery timelines vary. Additionally, incorporating predictive tools, such as Forecast-Informed Reservoir Operations (FIRO), could enhance the ability to balance water storage with downstream ecological needs amid fluctuating hydrological conditions [88]. By emphasizing future climate scenarios, this study highlights the need for adaptive reservoir operations and targeted restoration efforts, such as strategic riparian planting and sediment control measures, to mitigate the impacts of warming on stream temperatures and increased turbidity. The scalable nature of this framework supports the development of proactive, data-driven water resource management practices that address the intensifying impacts of wildfires and climate change on water quality.

4. Conclusions

This study provides a detailed assessment of wildfire and climate change impacts on stream temperature and turbidity in the Clackamas and Russian River Watersheds, United States, demonstrating the value of machine learning models in predicting post-fire water quality changes. By employing Random Forest (RF) and Support Vector Regression (SVR),

we investigated the complex interactions between climatic variables and hydrological responses, with RF models outperforming SVR due to their ability to handle non-linear relationships and identify key predictors. For example, RF achieved an R^2 of 0.98 and a root mean square error (RMSE) of 0.88 °C for stream temperature at the Estacada gauge in the Clackamas Watershed, compared to 0.97 and 1.09 °C, respectively, for SVR. Similarly, RF reduced turbidity prediction errors by over 15% compared to SVR at sites influenced by high post-fire sediment loads. Sensitivity analysis revealed that the 7-day average daily maximum air temperature and mean discharge were the most influential predictors, reflecting the role of short-term thermal dynamics and streamflow variability. Our comparison of nested watersheds highlights how smaller watersheds with higher burn percentages (e.g., 18% at Hopland) are more susceptible to stream temperature increases of up to 2.2 °C under RCP 8.5 and turbidity spikes exceeding 70 NTU during storm events.

The study findings provide valuable insights for localized adaptive water management strategies. While the study focuses on two distinct watersheds, the framework can be adapted to other regions facing similar challenges, offering a scalable approach for assessing post-fire water quality dynamics across various hydrological settings. Future research could further refine this framework by applying it to watersheds with diverse climatic and land-use conditions to evaluate its generalizability. Incorporating time-varying post-fire recovery metrics, such as vegetation indices and soil moisture, can enhance long-term predictions of watershed recovery. Consistent water quality monitoring using high-frequency sensors remains essential for improving model calibration and validation. Overall, this study underscores the importance of data-driven tools for adaptive water resource management in wildfire-prone regions. By identifying key drivers of post-fire water quality and projecting future stream conditions under different climate scenarios, the models developed here support proactive strategies that enhance the resilience of water resources and ecosystems amid escalating wildfire and climate impacts.

Author Contributions: Conceptualization, J.C. and H.C.; Data curation, J.C. and H.C.; Formal analysis, J.C.; Funding acquisition, H.C.; Investigation, J.C. and H.C.; Methodology, J.C. and H.C.; Project administration, H.C.; Resources, H.C.; Software, J.C.; Supervision, H.C.; Validation, J.C.; Visualization, J.C.; Writing—original draft, J.C. and H.C.; Writing—review and editing, J.C. and H.C. All authors have read and agreed to the published version of the manuscript.

Abbreviations

The following abbreviations are used in this manuscript:

7dADM	7-day moving average of the daily maximum
CMIP5	Coupled Model Intercomparison Project Phase 5
MACA	Multivariate Adaptive Constructed Analogs
RCP	Representative Concentration Pathway
RF	Random Forest
SVR	Support Vector Regression
USGS	United States Geological Survey

References

1. Chen, J.; Chang, H. A review of wildfire impacts on stream temperature and turbidity across scales. *Prog. Phys. Geogr.* **2023**, *47*, 369–394. [CrossRef]
2. Murphy, S.F.; Writer, J.H.; McCleskey, R.B.; Martin, D.A. The role of precipitation type, intensity, and spatial distribution in source water quality after wildfire. *Environ. Res. Lett.* **2015**, *10*, 084007. [CrossRef]
3. Rhoades, C.C.; Nunes, J.P.; Silins, U.; Doerr, S.H. The influence of wildfire on water quality and watershed processes: New insights and remaining challenges. *Int. J. Wildland Fire* **2019**, *28*, 721–725. [CrossRef]
4. Hohner, A.K.; Cawley, K.; Oropeza, J.; Summers, R.S.; Rosario-Ortiz, F.L. Drinking water treatment response following a Colorado wildfire. *Water Res.* **2016**, *105*, 187–198. [CrossRef]
5. Pennino, M.J.; Leibowitz, S.G.; Compton, J.E.; Beyene, M.T.; LeDuc, S.D. Wildfires can increase regulated nitrate, arsenic, and disinfection byproduct violations and concentrations in public drinking water supplies. *Sci. Total Environ.* **2022**, *804*, 149890. [CrossRef] [PubMed]
6. Smith, H.G.; Sheridan, G.J.; Lane, P.N.J.; Nyman, P.; Haydon, S. Wildfire effects on water quality in forest catchments: A review with implications for water supply. *J. Hydrol.* **2011**, *396*, 170–192. [CrossRef]
7. Jumps, N.; Gray, A.B.; Guilinger, J.J.; Cowger, W.C. Wildfire impacts on the persistent suspended sediment dynamics of the Ventura River, California. *J. Hydrol. Reg. Stud.* **2022**, *41*, 101096. [CrossRef]
8. Writer, J.H.; Hohner, A.; Oropeza, J.; Summers, R.S.; Rosario-Ortiz, F.L. Water treatment implications after the High Park Wildfire, Colorado. *J. Am. Water Works Assoc.* **2014**, *106*, E189–E199. [CrossRef]
9. Bladon, K.D.; Emelko, M.B.; Silins, U.; Stone, M. Wildfire and the future of water supply. *Environ. Sci. Technol.* **2014**, *48*, 8936–8943. [CrossRef] [PubMed]
10. Chang, H.; Watson, E.; Strecker, A. Climate change and stream temperature in the Willamette River Basin: Implications for fish habitat. In *World Scientific Series on Asia-Pacific Weather and Climate*; World Scientific: Singapore, 2018; pp. 119–132. [CrossRef]
11. Koontz, E.D.; Steel, E.A.; Olden, J.D. Stream thermal responses to wildfire in the Pacific Northwest. *Freshw. Sci.* **2018**, *37*, 731–746. [CrossRef]
12. Snover, A.K.; Whitely Binder, L.; Lopez, J.; Willmott, E.; Kay, J.; Howell, D.; Simmonds, J. Climate change impacts on water management in the Puget Sound region, Washington State, USA. *Water Res.* **2019**, *150*, 307–318. [CrossRef]
13. Webb, B.W.; Clack, P.D.; Walling, D.E. Water-air temperature relationships in a Devon river system and the role of flow. *Hydrol. Process.* **2008**, *17*, 3069–3084. [CrossRef]
14. Neitsch, S.L.; Arnold, J.G.; Kiniry, J.R.; Williams, J.R. *Soil and Water Assessment Tool Theoretical Documentation Version 2009*; Texas Water Resources Institute Technical Report No. 406; Texas Water Resources Institute: College Station, TX, USA, 2011. Available online: https://oaktrust.library.tamu.edu/items/ee261b66-c392-40d9-8c03-e455f5a8347e (accessed on 22 January 2025).
15. Verma, S.K.; Prasad, A.D.; Verma, M.K. An Assessment of ongoing developments in water Resources Management incorporating SWAT Model: Overview and Perspectives. *Nat. Environ. Pollut. Technol.* **2022**, *21*, 1963–1970. [CrossRef]
16. Kang, H.; Cole, R.P.; Miralha, L.; Compton, J.E.; Bladon, K.D. Hydrologic responses to wildfires in western Oregon, USA. *J. Hydrol.* **2024**, *639*, 131612. [CrossRef]
17. Rajesh, M.; Rehana, S. Prediction of river water temperature using machine learning algorithms: A tropical river system of India. *J. Hydroinform.* **2021**, *23*, 605–626. [CrossRef]
18. Wade, J.; Kelleher, C.; Hannah, D.M. Machine learning unravels controls on river water temperature regime dynamics. *J. Hydrol.* **2023**, *623*, 129821. [CrossRef]
19. Feigl, M.; Lebiedzinski, K.; Herrnegger, M.; Schulz, K. Machine-learning methods for stream water temperature prediction. *Hydrol. Earth Syst. Sci.* **2021**, *25*, 2951–2977. [CrossRef]
20. Culler, E.S.; Livneh, B.; Rajagopalan, B.; Tiampo, K.F. A data-driven evaluation of post-fire landslide susceptibility. *Nat. Hazards Earth Syst. Sci.* **2023**, *23*, 1631–1652. [CrossRef]
21. Shortridge, J.E.; Guikema, S.D.; Zaitchik, B.F. Machine learning methods for empirical streamflow simulation: A comparison of model accuracy, interpretability, and uncertainty in seasonal watersheds. *J. Hydrol.* **2016**, *532*, 67–78. [CrossRef]
22. Kisi, O.; Shiri, J.; Zounemat-Kermani, M.; Emamgholizadeh, S. Streamflow prediction using artificial intelligence techniques: An application to Kizilirmak River, Turkey. *J. Hydrol.* **2018**, *564*, 88–103. [CrossRef]
23. Basso, M.; Serpa, D.; Mateus, M.; Keizer, J.J.; Vieira, D.C.S. Advances on water quality modeling in burned areas: A review. *PLoS Water* **2022**, *1*, e0000025. [CrossRef]
24. Li, H.; Leung, L.R.; Tesfa, T.; Voisin, N.; Hejazi, M.; Liu, L.; Liu, Y.; Rice, J.; Wu, H.; Yang, X. Modeling stream temperature in the Anthropocene: An earth system modeling approach. *J. Adv. Model. Earth Syst.* **2015**, *7*, 1661–1679. [CrossRef]
25. Abatzoglou, J.T.; Williams, A.P. Impact of anthropogenic climate change on wildfire across western US forests. *Proc. Natl. Acad. Sci. USA* **2016**, *113*, 11770–11775. [CrossRef] [PubMed]
26. Westerling, A.L. Increasing western US forest wildfire activity: Sensitivity to changes in the timing of spring. *Philos. Trans. R. Soc. B Biol. Sci.* **2016**, *371*, 20150178. [CrossRef]

27. Chen, J.; Chang, H. Relative impacts of climate change and land cover change on streamflow using SWAT in the Clackamas River Watershed, USA. *J. Water Clim. Change* **2021**, *12*, 1454–1470. [CrossRef]

28. Krochta, M.; Chang, H. Scales of connectivity within stream temperature networks of the Clackamas River Basin, Oregon. *Ann. Am. Assoc. Geogr.* **2024**, *114*, 1653–1667. [CrossRef]

29. Long, W.B.; Chang, H. Event scale analysis of streamflow response to wildfire in Oregon, 2020. *Hydrology* **2022**, *9*, 157. [CrossRef]

30. Newcomer, M. Storm and annual time scale hydrological data for the Russian River Watershed 1996–2022 [Dataset]. In *OSTI OAI*; U.S. Department of Energy Office of Scientific and Technical Information: Oak Ridge, TN, USA, 2022. [CrossRef]

31. Johnson, S.L.; Gómez-Pujol, L.; Fornós, J.; Del Valle, L.; Nogales, B. Flood risk and sediment transport in the Russian River Watershed. *Geomorphology* **2016**, *287*, 1–14. [CrossRef]

32. Opperman, J.J.; Lohse, K.A.; Brooks, C.; Kelly, N.M.; Merenlender, A.M. Influence of land use on fine sediment in salmonid spawning gravels within the Russian River Basin, California. *Can. J. Fish. Aquat. Sci.* **2005**, *62*, 2740–2751. [CrossRef]

33. Sumargo, E.; Steele-Dunne, S.C.; De Lannoy, G.J.M. Understanding the hydrologic impact of atmospheric rivers in the Russian River Watershed. *J. Hydrometeorol.* **2020**, *21*, 123–137. [CrossRef]

34. Jaramillo, F. Influence of groundwater dynamics on stream water quality in the Russian River Watershed. *Hydrol. Process.* **2012**, *26*, 3692–3700. [CrossRef]

35. Newcomer, M.E.; Underwood, J.; Murphy, S.F.; Ulrich, C.; Schram, T.; Maples, S.R.; Peña, J.; Siirila-Woodburn, E.R.; Trotta, M.; Jasperse, J.; et al. Prolonged drought in a northern California coastal region suppresses wildfire impacts on hydrology. *Water Resour. Res.* **2023**, *59*, e2022WR034206. [CrossRef]

36. PRISM Climate Group. High-Resolution Spatial Climate Data for the United States. Oregon State University. Available online: http://prism.oregonstate.edu (accessed on 15 September 2023).

37. Abatzoglou, J.T.; Brown, T.J. Multivariate Adaptive Constructed Analogs (MACA) Downscaled Climate Dataset. Available online: https://climate.northwestknowledge.net/MACA/ (accessed on 7 March 2024).

38. Isaak, D.J.; Wollrab, S.; Horan, D.; Chandler, G. Climate change effects on stream and river temperatures across the northwest U.S. from 1980–2009 and implications for salmonid fishes. *Clim. Change* **2012**, *113*, 499–524. [CrossRef]

39. Steel, E.A.; Tillotson, A.; Larsen, D.A.; Fullerton, A.H.; Denton, K.P.; Beckman, B.R. Beyond the mean: The role of variability in predicting ecological responses to stream temperature increases. *Ecosphere* **2016**, *7*, e01251. [CrossRef]

40. Mohseni, O.; Stefan, H.G.; Eaton, J.G. Global warming and potential changes in fish habitat in US streams. *Clim. Change* **2003**, *59*, 389–409. [CrossRef]

41. Arismendi, I.; Johnson, S.L.; Dunham, J.B.; Haggerty, R.; Hockman-Wert, D. The paradox of cooling streams in a warming world: Regional climate trends do not parallel variable local trends in stream temperature in the Pacific continental United States. *Geophys. Res. Lett.* **2014**, *41*, 5295–5305. [CrossRef]

42. Croke, J.; Wallbrink, P.; Fogarty, P.; Mockler, S.; McCormack, B.; Brophy, J. Managing sediment sources and movement in forests: The forest industry and water quality. *Aust. For.* **1999**, *62*, 14–20. Available online: http://worldcat.org/isbn/1876006552 (accessed on 22 January 2025).

43. Lane, P.N.J.; Sheridan, G.J.; Noske, P.J.; Sherwin, C.B. Phosphorus and nitrogen exports from SE Australian forests following wildfire. *J. Hydrol.* **2006**, *331*, 150–161. [CrossRef]

44. Moody, J.A.; Martin, D.A. Initial hydrologic and geomorphic response following a wildfire in the Colorado Front Range. *Earth Surf. Process. Landf.* **2001**, *26*, 1049–1070. [CrossRef]

45. Rust, A.J.; Saxe, S.; McCray, J.; Rhoades, C.C.; Hogue, T.S. Evaluating the factors responsible for post-fire water quality response in forests of the western USA. *Int. J. Wildland Fire* **2019**, *28*, 769–783. [CrossRef]

46. Chen, H.J.; Chang, H. Response of discharge, TSS, and E. coli to rainfall events in urban, suburban, and rural watersheds. *Environ. Sci. Process. Impacts* **2014**, *16*, 2313–2324. [CrossRef] [PubMed]

47. Chen, J.; Chang, H. Dynamics of wet-season turbidity in relation to precipitation, discharge, and land cover in three urbanizing watersheds. *Oregon. River Res. Appl.* **2019**, *35*, 892–904. [CrossRef]

48. Robichaud, P.R.; Wagenbrenner, J.W.; Brown, R.E.; Wohlgemuth, P.M. Post-fire rehabilitation treatments: Controlling soil erosion and mitigating post-fire effects on runoff and sediment yields. In *Post-Fire Management and Restoration of Southern European Forests*; Springer: Dordrecht, The Netherlands, 2013; pp. 155–170. [CrossRef]

49. Neary, D.G.; Ryan, K.C.; DeBano, L.F. (Eds.) *Wildland Fire in Ecosystems: Effects of Fire on Soil and Water*; U.S. Department of Agriculture, Forest Service, Rocky Mountain Research Station: Ogden, UT, USA, 2005. [CrossRef]

50. Saxe, S.; Hogue, T.S.; Hay, L. Characterization and evaluation of controls on post-fire streamflow response across western US watersheds. *Hydrol. Earth Syst. Sci.* **2023**, *22*, 1221–1237. [CrossRef]

51. Emelko, M.B.; Silins, U.; Bladon, K.D.; Stone, M. Implications of land disturbance on drinking water treatability in a changing climate: Demonstrating the need for "source water supply and protection" strategies. *Water Res.* **2011**, *45*, 461–472. [CrossRef] [PubMed]

52. Breiman, L. Random forests. *Mach. Learn.* **2001**, *45*, 5–32. [CrossRef]

53. Blöschl, G.; Sivapalan, M.; Wagener, T.; Viglione, A.; Savenije, H. *Runoff Prediction in Ungauged Basins: Synthesis Across Processes, Places and Scales*; Cambridge University Press: Cambridge, UK, 2013. [CrossRef]

54. Saltelli, A.; Ratto, M.; Andres, T.; Campolongo, F.; Cariboni, J.; Gatelli, D.; Tarantola, S. *Global Sensitivity Analysis: The Primer*; John Wiley & Sons: Chichester, UK, 2004.

55. Campolongo, F.; Cariboni, J.; Saltelli, A. An effective screening design for sensitivity analysis of large models. *Environ. Model. Softw.* **2007**, *22*, 1509–1518. [CrossRef]

56. Gupta, H.V.; Razavi, S. Revisiting the basis of sensitivity analysis for dynamical earth system models. *Water Resour. Res.* **2018**, *54*, 8692–8717. [CrossRef]

57. Pianosi, F.; Sarrazin, F.; Wagener, T. A Matlab toolbox for global sensitivity analysis. *Environ. Model. Softw.* **2020**, *104*, 120–133. [CrossRef]

58. Razavi, S.; Gupta, H.V. A new framework for comprehensive, robust, and efficient global sensitivity analysis: 1. Theory. *Water Resour. Res.* **2016**, *52*, 423–439. [CrossRef]

59. Zema, D.A.; Mancuso, M.; Zimbone, S.M.; Giordano, G.; Smeriglio, A.; Randazzo, L.; Chimenti, L. Modeling surface runoff and soil erosion after prescribed fires: Effectiveness of Random Forest models. *Environ. Sci. Pollut. Res.* **2024**, *31*, 12345–12360. [CrossRef]

60. Folharini, S.; Vieira, A.; Bento-Gonçalves, A.; Silva, S.; Marques, T.; Novais, J. Soil erosion quantification using machine learning in sub-watersheds of Northern Portugal. *Hydrology* **2023**, *10*, 7. [CrossRef]

61. Aguilera, R.; Luo, N.; Basu, R.; Wu, J.; Clemesha, R.; Gershunov, A.; Benmarhnia, T. A novel ensemble-based statistical approach to estimate daily wildfire-specific $PM_{2.5}$ in California (2006–2020). *Environ. Int.* **2023**, *171*, 107719. [CrossRef]

62. Sharma, B.; Goel, N.K. Streamflow prediction using support vector regression machine learning model for Tehri Dam. *Appl. Water Sci.* **2024**, *14*, 99. [CrossRef]

63. Asefa, T.; Kemblowski, M.; McKee, M.; Khalil, A. Multi-time scale streamflow predictions: The support vector machines approach. *J. Hydrol.* **2006**, *318*, 7–16. [CrossRef]

64. Khan, M.T.; Coulibaly, P. Application of support vector machine in lake water level prediction. *J. Hydrol. Eng.* **2006**, *11*, 199–205. [CrossRef]

65. Yu, P.S.; Chen, S.T.; Chang, L.C. Support vector regression for real-time flood stage forecasting. *J. Hydrol.* **2016**, *328*, 704–716. [CrossRef]

66. Abrahart, R.J.; Anctil, F.; Coulibaly, P.; Dawson, C.W.; Mount, N.J.; See, L.; Wilby, R.L. Two decades of anarchy? Emerging themes and outstanding challenges for neural network river forecasting. *Prog. Phys. Geogr.* **2012**, *36*, 480–513. [CrossRef]

67. Lerios, J.L.; Villarica, M.V. Pattern extraction of water quality prediction using machine learning algorithms of water reservoir. *Int. J. Mech. Eng. Robot.* **2019**, *8*, 992–997. [CrossRef]

68. Null, S.E.; Viers, J.H.; Mount, J.F. Hydrologic response and watershed sensitivity to climate warming in California's Sierra Nevada. *PLoS ONE* **2013**, *8*, e56854. [CrossRef]

69. Folador, L.; Cislaghi, A.; Vacchiano, G.; Masseroni, D. Integrating remote and in-situ data to assess the hydrological response of a post-fire watershed. *Hydrology* **2021**, *8*, 169. [CrossRef]

70. Soulis, K.X.; Generali, K.A.; Papadaki, C.; Theodoropoulos, C.; Psomiadis, E. Hydrological response of natural Mediterranean watersheds to forest fires. *Hydrology* **2021**, *8*, 15. [CrossRef]

71. Criminisi, A.; Shotton, J.; Konukoglu, E. Decision forests: A unified framework for classification, regression, density estimation, manifold learning and semi-supervised learning. *Found. Trends Comput. Graph. Vis.* **2012**, *7*, 81–227. [CrossRef]

72. Smola, A.J.; Schölkopf, B. A tutorial on support vector regression. *Stat. Comput.* **2004**, *14*, 199–222. [CrossRef]

73. Graham, D.J.; Bierkens, M.F.; Van Vliet, M.T. Impacts of droughts and heatwaves on river water quality worldwide. *J. Hydrol.* **2024**, *629*, 130590. [CrossRef]

74. Cooper, S.D.; Page, H.M.; Wiseman, S.W.; Klose, K.; Bennett, D.; Even, T.; Sadro, S.; Nelson, C.E.; Dudley, T.L. Physicochemical and biological responses of streams to wildfire severity in riparian zones. *Freshw. Biol.* **2014**, *60*, 2600–2619. [CrossRef]

75. Meng, R.; Dennison, P.E.; Huang, C.; Moritz, M.A.; D'Antonio, C. Effects of fire severity and post-fire climate on short-term vegetation recovery of mixed-conifer and red fir forests in the Sierra Nevada Mountains of California. *Remote Sens. Environ.* **2015**, *171*, 311–325. [CrossRef]

76. Zhou, Y.; Wehner, M.; Collins, W. Back-to-back high category atmospheric river landfalls occur more often on the west coast of the United States. *Commun. Earth Environ.* **2024**, *5*, 187. [CrossRef]

77. Rathburn, S.L.; Shahverdian, S.M.; Ryan, S.E. Post-disturbance sediment recovery: Implications for watershed resilience. *Geomorphology* **2018**, *305*, 61–75. [CrossRef]

78. Clifton, C.F.; Day, K.T.; Luce, C.H.; Grant, G.E.; Safeeq, M.; Halofsky, J.E.; Staab, B.P. Effects of climate change on hydrology and water resources in the Blue Mountains, Oregon, USA. *Clim. Serv.* **2018**, *10*, 9–19. [CrossRef]

79. Beyene, M.T.; Leibowitz, S.G. Heterogeneity in post-fire thermal responses across Pacific Northwest streams: A multi-site study. *J. Hydrol. X* **2024**, *23*, 100173. [CrossRef] [PubMed]

80. Swartz, A.; Warren, D. Wildfire in western Oregon increases stream temperatures, benthic biofilms, and juvenile coastal cutthroat trout size and densities with mixed effects on adult trout and coastal giant salamanders. *Can. J. Fish. Aquat. Sci.* **2022**, *80*, 503–516. [CrossRef]

81. Wootten, A.; Terando, A.; Reich, B.J.; Boyles, R.P.; Semazzi, F. Characterizing sources of uncertainty from global climate models and downscaling techniques. *J. Appl. Meteorol. Climatol.* **2017**, *56*, 3245–3262. [CrossRef]

82. Giorgi, F. Uncertainties in climate change projections, from the global to the regional scale. *EPJ Web Conf.* **2010**, *9*, 115–129. [CrossRef]

83. Yimer, S.M.; Bouanani, A.; Kumar, N.; Tischbein, B.; Borgemeister, C. Assessment of climate models performance and associated uncertainties in rainfall projection from CORDEX over the Eastern Nile Basin, Ethiopia. *Climate* **2022**, *10*, 95. [CrossRef]

84. Ghosh, S.; Mujumdar, P.P. Nonparametric methods for modeling GCM and scenario uncertainty in drought assessment. *Water Resour. Res.* **2007**, *43*, 7. [CrossRef]

85. Kuhn, M.; Johnson, K. *Applied Predictive Modeling*; Springer: New York, NY, USA, 2013.

86. Qiu, R.; Wang, D.; Singh, V.P.; Wang, Y.; Wu, J. Integration of deep learning and improved multi-objective algorithm to optimize reservoir operation for balancing human and downstream ecological needs. *Water Res.* **2024**, *253*, 121314. [CrossRef] [PubMed]

87. Zhuang, Y.; Fu, R.; Lisonbee, J.; Sheffield, A.M.; Parker, B.A.; Deheza, G. Anthropogenic warming has ushered in an era of temperature-dominated droughts in the western United States. *Sci. Adv.* **2024**, *10*, eadn9389. [CrossRef]

88. Delaney, C.J.; Hartman, R.K.; Mendoza, J.; Dettinger, M.; Delle Monache, L.; Jasperse, J.; Ralph, F.M.; Talbot, C.; Brown, J.; Reynolds, D.; et al. Forecast informed reservoir operations using ensemble streamflow predictions for a multipurpose reservoir in Northern California. *Water Resour. Res.* **2020**, *56*, e2019WR026604. [CrossRef]